NPS-OR-94-016

NAVAL POSTGRADUATE SCHOOL

Monterey, California

DTIC
ELECTE
FEB 15 1995
S D
B

STOCHASTIC MODELS FOR CELL SIGNALING AND TOXIC EFFECTS ON CELLS

D. P. Gaver
P. A. Jacobs
R. L. Carpenter
T. K. Narayanan

19950206 002

December 1994

Approved for public release; distribution is unlimited.

Prepared for:
Naval Medical Research Institute/Toxicology Detachment
Wright-Patterson Air Force Base, Ohio

NAVAL POSTGRADUATE SCHOOL
MONTEREY, CA 93943-5000

Rear Admiral T. A. Mercer
Superintendent

Harrison Shull
Provost

This report was prepared for and funded by the Naval Medical Research Institute/Toxicology Detachment, Wright-Patterson Air Force Base, Ohio .

Reproduction of all or part of this report is authorized.

This report was prepared by:

Donald P. Gaver
DONALD P. GAVER, JR.
Professor of Operations Research

Patricia A. Jacobs
PATRICIA A. JACOBS
Professor of Operations Research

Robt. L. Carpenter
ROBERT L. CARPENTER (by DPG)
Senior Scientist

T. K. Narayanan
TANDORE K. NARAYANAN (by DPG)
Staff Scientist

Reviewed by:

PETER PURDUE
Professor and Chairman
Department of Operations Research

Released by:

PAUL J. MARTO
Dean of Research

REPORT DOCUMENTATION PAGE

Form Approved
OMB No. 0704-0188

Public reporting burden for this collection of information is estimated to average 1 hour per response, including the time for reviewing instructions, searching existing data sources, gathering and maintaining the data needed, and completing and reviewing the collection of information. Send comments regarding this burden estimate or any other aspect of this collection of information, including suggestions for reducing this burden, to Washington Headquarters Services, Directorate for Information Operations and Reports, 1215 Jefferson Davis Highway, Suite 1204, Arlington, VA 22202-4302, and to the Office of Management and Budget, Paperwork Reduction Project (0704-0188), Washington, DC 20503.

1. AGENCY USE ONLY *(Leave blank)*	2. REPORT DATE	3. REPORT TYPE AND DATES COVERED
	December 1994	Technical

4. TITLE AND SUBTITLE
Stochastic Models for Cell Signaling and Toxic Effects on Cells

5. FUNDING NUMBERS

6. AUTHOR(S)
Donald P. Gaver, Patricia A. Jacobs, Robert L. Carpenter, and Tandore K. Narayanan

7. PERFORMING ORGANIZATION NAME(S) AND ADDRESS(ES)
Naval Postgraduate School
Monterey, CA 93943

8. PERFORMING ORGANIZATION REPORT NUMBER
NPS-OR-94-016

9. SPONSORING / MONITORING AGENCY NAME(S) AND ADDRESS(ES)
Naval Medical Research Institute/Toxicology Detachment
Wright-Patterson Air Force Base, OH 45433-6503

10. SPONSORING / MONITORING AGENCY REPORT NUMBER

11. SUPPLEMENTARY NOTES

12a. DISTRIBUTION / AVAILABILITY STATEMENT
Approved for public release; distribution is unlimited.

12b. DISTRIBUTION CODE

13. ABSTRACT *(Maximum 200 words)*

This paper presents generic models for the effect of a chemical toxin on cells forming the tissue of an organ. The models are illustrative, not specific to organ or toxin. Interactive response of within-tissue toxin and cells is modeled: cell capability to modify (metabolize or bind) toxin is represented, as is the alteration of that capability by toxin presence. Both processes are represented in the context of simple versions of the cell cycle.

Toxin-cell interaction is explicitly represented in terms of inter-cell chemical signaling that encourages replacement or repair of cells. The impact of cell death by apoptosis and necrosis is represented in terms of within-tissue toxin concentration. The model is explicitly stochastic, representing inter-cell and toxin input and within-organ concentration in terms of diffusion approximations. Explicit mathematical discussion is given of dose-response function behavior at low doses.

14. SUBJECT TERMS

DTIC QUALITY INSPECTED 4

15. NUMBER OF PAGES
71

16. PRICE CODE

17. SECURITY CLASSIFICATION OF REPORT	18. SECURITY CLASSIFICATION OF THIS PAGE	19. SECURITY CLASSIFICATION OF ABSTRACT	20. LIMITATION OF ABSTRACT
Unclassified	Unclassified	Unclassified	UL

STOCHASTIC MODELS FOR CELL SIGNALING AND TOXIC EFFECTS ON CELLS

D. P. Gaver and P. A. Jacobs
Department of Operations Research
Naval Postgraduate School
Monterey, CA 93943

R. L. Carpenter
Naval Medical Research Institute
Toxicology Detachment
Wright-Patterson Air Force Base, OH 45433-6503

T. K. Narayanan
Geo-Centers Inc.
Washington Operations
10903 Indian Head Highway
Ft. Washington, MD 20744

Abstract

This paper presents generic models for the effect of a chemical toxin on cells forming the tissue of an organ. The models are illustrative, not specific to organ or toxin. Interactive response of within-tissue toxin and cells is modeled: cell capability to modify (metabolize or bind) toxin is represented, as is the alteration of that capability by toxin presence. Both processes are represented in the context of simple versions of the cell cycle.

Toxin-cell interaction is explicitly represented in terms of inter-cell chemical signaling that encourages replacement or repair of cells. The impact of cell death by apoptosis and necrosis is represented in terms of within-tissue toxin concentration. The model is explicitly stochastic, representing inter-cell and toxin input and within-organ concentration in terms of diffusion approximations. Explicit mathematical discussion is given of dose-response function behavior at low doses.

1. Introduction

Application of laboratory toxicology data to environmental and human problems of risk assessment almost always requires extrapolation of the data from the experimentally-used dose regimen to the exposure conditions of practical concern, and from the animal species tested to the species of concern (usually man). This extrapolation and estimation process is known as *chemical risk assessment*. The risk assessment process has undergone considerable evolution, moving from a qualitative basis for decision making to an increasingly quantitative basis, and from the use of default assumptions to the application of mechanistic mathematical models as tools upon which to base decisions. In the context of determining safe human exposure limits to potentially toxic chemicals, there are two sub-tasks to be accomplished: estimation of low-dose risk in animals, and the subsequent conversion of animal risk estimates to human risk estimates. An authoritative survey of many of the statistical issues and opportunities is given by Krewski and Franklin (1991).

Extrapolation to low-dose effect, the first sub-task, can be accomplished either by assuming that biological response varies in a specified mathematical manner (e.g. probit, logit) with organ host exposure, or by using physiologically-based pharmacokinetic (PBPK) models to relate organ dose to host exposure; cf. Krewski and Franklin (1991), chapters 8 and 9; M. Andersen, H. Clewell Jr., and C. Travis have been prominent in this research area. In the latter approach, multi-compartment physiological models are formulated using actual tissue volumes from the experimental and target species and actual perfusion rates to provide for chemical transport between the compartments. Thus the pharmacokinetics of high to low-dose extrapolation become amenable to calculation, and external measures of external dose or exposure can be translated to concentrations in the

For
ed
tion
Availability Codes
Dist Avail and/or Special
A-1

target organ (internal dose). Target-organ chemical concentration may be translated into estimates of risk if a suitable biologically acceptable mathematical model can be used to relate chemical presence in the organ to harmful outcome. Such models, called pharmacodynamic, exist for carcinogens, in the form of the widely-used linearized multistage approximation for cancer dose/response, and multistage clonal expansion models; cf. Moolgavkar (1988). These models are based on the general concept that chemical alteration of the cellular genes may give rise to permanent, heritable changes in the genetic information stored in the cell nucleus, and lead to phenotypic changes in the altered cells that ultimately cause the formation of malignant tumors. Simulation is sometimes used to study stochastic models of carcinogenesis for large numbers of cells; (cf. Bois (1992)).

Unfortunately, analogous dose/response models are not widely available for toxic responses other than carcinogenesis. The mathematical expression of even the relatively simple concept of genetic alteration leading to cancer involves significant simplification of biological reality, and significant mathematical complexity. This state of affairs is exacerbated when one attempts to describe the interactions leading to loss of cell function and cell death in tissues of a whole animal. The multi-layered control and response systems present in an intact living animal are poorly understood and thus have not yet been adequately modeled. Nonetheless, these control mechanisms defend against the majority of toxic effects observed as a result of chemical exposure, and their failure represents much of what is observed as the expression of toxicity.

This paper describes initial formulations of models for cellular response to toxic insult. Beginning with a simple Markov model, successive models increase in biological resolution or refinement as well as mathematical complexity. Our model formulation takes into account broad aspects of the current state of

knowledge concerning the control and regulation of cellular properties in tissue. The design of these models is not to provide a detailed description of the response of specific organs to toxic insult, but rather to begin the process of mathematically describing recent significant advances in knowledge that have been made in cell biology, hormonal regulation, and hormetic control mechanisms that regulate cell response to toxicants. Some modifications of the model formulations may be needed to apply them to specific organs; for one thing the complex geometry of organ architecture is not represented. To have included complex, three-dimensional relationships between different cell types would have increased the mathematical complexity considerably. But even in its present rudimentary state the model is useful for stimulating discussion and suggesting experimentation, with the goal of furthering the understanding of cellular response to toxic substances including the effects of tissue-mediated responses (e.g. mitogenic stimulation). The current formulation of the model, or extensions thereof, is suitable for experimental evaluation in cell culture if the experimental conditions are properly chosen and chemical-specific details are added.

We provide the following abbreviated biological background. The tissue making up organs almost always involves a complex geometrical juxtaposition of several cell types having specific and often overlapping functions. This tissue architecture may be maintained by the presence of a nonliving matrix of proteins collectively known as a *basement membrane*. Interactions between this membrane and the cells are known to be critical to its stability as a mature, functioning entity. The whole of the tissue is permeated by branching blood vessels, each generation of which is successively smaller; these serve to provide a constant, stable milieu in which the cells exist. Nutrients, control signals in the form of specific biomolecules, and xenobiotic chemicals are brought to the immediate

surroundings of the cell by the vasculature in the tissue and cellular metabolic products; the products of energy metabolism and cellularly derived control biomolecules are removed from the cellular microenvironment by the same means.

The state of the cell at any time is a reflection of its age, the summation of the control chemicals reaching and leaving the cell, the effects of xenobiotic chemicals present, if any, and the state of the cells surrounding it. Cellular contact with the surrounding cells and basement membrane act to supply chemical signals that modulate its activity. A given cell may be (i) nearly quiescent, (ii) active biochemically, i.e., producing metabolites of absorbed materials for its own use or for export, (iii) in a state of stress due to shortage or excess of biochemical molecules, (iv) in a process of programmed cell death (apoptosis), (v) in the process of dying from chemical insult (necrosis), or (vi) dividing to form progenitor cells in response to a need to replace cells already lost; these conditions need not be mutually exclusive at any point in time. Some specific cells may alter or completely change their observable characteristics in response to chemical signals. The most well-known of these cells are the pluripotent stem cells of the hematopoietic system.

The models to be presented here represent some, but by no means all, of the features mentioned. They provide a basis for proceeding further.

2. Model Structure

In the following sections of this paper we present a sequence of mathematical models that represent interactions between the cells in an organ's tissue and a toxic chemical or agent (hereafter called *toxin*) originating externally and entering the organ and coming into contact with the cells, possibly in modified form. The initial models postulate a mature organ with capacity to contain, at most, a fixed

number of cells. Broadly speaking, the organ's cells attempt to remove (e.g. metabolize or bind) the toxin, but are, to a dose-dependent degree, also affected by the toxin concentration. We distinguish between cells that are in one of two stages of the cell cycle: these we call, oversimplifying the true cell cycle, *functional*, and *dividing* (S-phase and mitotic). Functional cells are assumed to be capable of removing toxin, but are also susceptible to premature death because of the toxin's action. Dividing cells are in the process of DNA replication and actual mitosis, here splitting into two daughter cells; while in this stage the cells are assumed incapable of removing toxin. However, toxin presence is assumed to affect the cell cycle, e.g. by shortening the functional, and lengthening the dividing, stages. The model proposed emphasizes inter-cellular signaling: when a cell dies, i.e. ceases to function, it effectively requests one other functioning cell to divide to produce its replacement. It is biologically plausible that signaling occurs only to neighboring cells, but the present model, being without spatial characteristics, does not literally recognize this restriction. Also, signals are assumed to be specific: one signal is emitted per cell death, so eventually one replacement occurs. Alternative formulations are sometimes plausible and are easily studied.

3. Single-Stage Markov Model

We now present several alternative simple Markov models for cell-toxin interaction, emphasizing the representation of signaling. Although cells can age and exist in different stages of functionality we omit an account of this at first, but return to it later.

Let $D(t)$ represent the number of functional cells in the organ at time t, and $M(t)$ the number of dividing (mitotic) cells. If a functioning cell that dies immediately induces another to begin division (instant signaling) then

$$C_0 = D(t) + 2M(t) \tag{3.1}$$

where C_0 is the maximum organ size, here assumed constant; realistic elaborations are possible. Note that organ size is, strictly speaking, $D(t) + M(t)$, which is the number of cells present at time t; C_0 acknowledges that space for all cells must leave room for each cell currently in mitosis to eventually become two differentiated cells. We describe $\{D(t), M(t)\}$ as a birth and death process in continuous time, with $D(t) \in (0, 1, 2, \ldots, C_0)$. Typically C_0 is large, i.e. of order 10^{10}–10^{12} for mature humans, and this will be exploited to carry out an asymptotic analysis.

Let $T(t)$ denote the concentration of toxin in the organ at time t. We represent $\{T(t)\}$ as a diffusion process whose drift and diffusion coefficients are both influenced by $D(t)$ so as to represent metabolic or binding action, hence toxin removal, and by the toxin input to the organ, $\tau(t)$, as well as the instantaneous concentration, $T(t)$, itself.

In the following we describe specific models, beginning with the most simple and (potentially) least realistic, but also the most parsimonious. We explicitly include the effect of inter-cellular signaling.

3.1 Cellular Signaling

Suppose a cell dies from some cause: apoptosis or necrosis. The effect of its signaling to other cells for replacement can be captured by postulating that a *ghost* (release of growth factor) of the newly-dead cell now exists, the function of which is to find and interact with a neighboring live cell, inducing that cell to divide. The ghost then disappears after its purpose is served. One can thus represent the delay in mitotic response to cell death by adjusting the ghost's search rate for functional cells.

The following describes a possible Markov generator that includes the signaling (ghost) influence. Let $G(t)$ denote the number of signals present in the organism at time t, and introduce the constraint

$$C_0 = D(t) + G(t) + 2M(t). \tag{3.2}$$

The following then describes the possible transitions allowed to occur in a small time interval, $(t, t + dt)$.

Signaling Model
(Markov Generator)

t		$t + dt$	*Probability*
$D(t), G(t), M(t);$ $T(t)$	$\rightarrow$	$D(t) - 1, G(t) + 1, M(t)$ $T(t) + \delta^* dt + \sigma dW(t)$ (cell death, signal creation)	$\lambda^* D(t) dt$
	$\rightarrow$	$D(t) - 1, G(t) - 1, M(t) + 1$ $T(t) + \delta^* dt + \sigma dW(t)$ (cell signaled to divide, signal disappears)	$\theta^* G(t)(D(t)/C_0) dt$
	$\rightarrow$	$D(t) + 2, G(t), M(t) - 1$ $T(t) + \delta^* dt + \sigma dW(t)$ (two newly-divided cells emerge)	$\mu^* M(t)\, dt$

(3.3)

All rates of cell transition, namely λ^*, θ^*, and μ^* are presumed to be influenced by current toxin concentration, $T(t)$. In turn, the latter is influenced by the metabolic or binding capability of the cells to remove toxin; the net mean increase of toxin in the short run is $\delta^*(T(t), D(t), \tau(t))$. Our subsequent analysis does not, in principle, depend upon specific functional forms for any of the above parameters; adequate smoothness and differentiability is assumed where necessary. When specific functions are required we shall use these:

$$\lambda^*(T(t)) = \lambda_0 e^{\lambda^* T(t)} \tag{3.4,a}$$

$$\mu^*(T(t)) = \mu_0 e^{-\mu^* T(t)} \tag{3.4,b}$$

$$\theta^*(T(t)) = \theta_0 e^{-\theta^* T(t)}; \quad \lambda^*, \theta^*, \mu^* > 0. \tag{3.4,c}$$

Note that it has been assumed that increased toxin level increases cell death rate, decreases the rate of completing mitosis, and slows the rate at which ambient signals reach their destinations. The net effect is to reduce the number of functional cells. All of the above dependencies are hypothetical and illustrative only. In particular

$$\delta^*\left(T(t), D(t), \tau^*(t)\right) = \left(\tau^*(t) - \nu^* \frac{T(t)(D(t)/C_0)}{1+\kappa^* T(t)}\right) \tag{3.5}$$

where in the latter $\tau^*(t)$ represents toxin input rate to the organ, and the remaining term $\nu^*(T(t)D(t)/C_0)/\left[1+\kappa^* T(t)\right]$ represents the toxin concentration rate-limited (Michaelis-Menton) reduction by functional cells.

It has been observed that the realistic effect of toxin presence on λ^*, μ^*, θ^*, etc. at time t may involve the entire past history of such exposure, e.g. $\lambda^*(t) = \lambda^*(T(x), a \le x \le t)$; the explicit function may be illustrated by the form $\lambda^*(t) = \exp\left[\int_0^t \lambda^*(T(x)dx)\right]$. A further model enhancement would recognize that toxin presence in the organ may result in cells that complete completing mitosis giving rise to damaged cells, e.g. possessing DNA adducts. These cells now become susceptible to repair.

3.2 Differential Equations For Deterministic Approximations

Let C_0 denote the number of spaces/holes that cells may occupy. Then

$$C_0 = D(t) + G(t) + 2M(t) \tag{3.6}$$

since the cells in division potentially require two holes. Assume that if $C_0 >> 1$ then

$$D(t)/C_0 \to \alpha(t),\ G(t)/C_0 \to \gamma(t),\ T(t)/C_0 \to \beta(t) \tag{3.7}$$

in probability as $C_0 \to \infty$ where the latter functions are O(1). The following differential equations result from direct manipulation of (3.3):

$$\frac{d\alpha(t)}{dt} = -\lambda\alpha(t) - \theta\alpha(t)\gamma(t) + 2\mu\left(1-\alpha(t)-\gamma(t)\right)\frac{1}{2}; \tag{3.8}$$

the last term occurs by virtue of (3.6). Also,

$$\frac{d\gamma(t)}{dt} = \lambda\alpha(t) - \theta\alpha(t)\gamma(t) \tag{3.9}$$

$$\frac{d\beta}{dt} = \delta = \tau - \frac{\nu\alpha\beta}{1+\kappa\beta} \tag{3.10}$$

We re-emphasize that all parameters are implicit functions of (current) toxin level, $T(t)$, and possibly also absolute time, t, which can be viewed as the age of a mature organ, rather than an individual cell. This latter step is not taken in this paper.

Note that in (3.8), (3.9), (3.10) the original parameters of (3.3) must be scaled: $\lambda^*(T(t))$ is replaced by $\lambda(\beta(t))$, $\theta^*(T(t))$ by $\theta(\beta(t))$, $\mu^*(T(t))$ by $\mu(\beta(t))$, $\nu^*(T(t))$ by $\nu(\beta(t))$, τ^* by τC_0, and κ^* by κC_0.

In Section 6 such scaling is exploited more extensively to deduce stochastic behavior of system state values.

3.3 Solution Without Toxin Input

Suppose no toxin input exists, so $T(t) = 0$, $\forall t \geq 0$. Then a steady-state solution to (3.8) and (3.9) may occur: set derivatives = 0 and solve the resulting equations to find

$$\gamma = \frac{\lambda}{\theta}, \quad \text{provided} \quad 0 \leq \frac{\lambda}{\theta} < 1 \tag{3.11}$$

$$\alpha = \frac{\mu(1-\lambda/\theta)}{2\lambda+\mu}. \tag{3.12}$$

The latter implies (i) that the larger the signal activity rate, θ, the smaller the ambient signal population, and the more quickly does signaling induce another cell to begin division; furthermore (ii) if $\theta >> \lambda$, the death rate, signifying highly efficient signaling, then $\alpha \to \mu/(2\lambda + \mu)$, which is equivalent to thinking of cells as behaving in *pairs*: once division completes the two daughters effectively compete to die (rate 2λ).

Although the equations (3.8) and (3.9) are non-linear and apparently cannot be solved explicitly one can obtain an approximate time-dependent solution as follows:

(a) assume $\gamma(t)$ quickly reaches steady state, so

$$\gamma(t) \equiv \lambda/\theta; \quad 0 < t \tag{3.13}$$

This is a standard and useful approximation technique often invoked in biochemical kinetics problems that is variously abbreviated the *quasi-steady-state assumption* (QSSA) or the *pseudo-steady-state hypothesis* (PSSH); see Segel and Slemrod (1989) for a careful exposition of its rationale. The QSSA approach gives rise to the classical Michaelis-Menton used widely in pharmaceutical kinetics and compartment models; it already appears implicitly in our (3.5) and (3.10).

(b) introduce (3.13) into (3.8) to find the approximation $\tilde{\alpha}(t)$:

$$d\tilde{\alpha}(t)/dt = -(2\lambda+\mu)\alpha + \mu(1-\lambda/\theta), \tag{3.14}$$

the solution of which is

$$\begin{aligned}\tilde{\alpha}(t) &= \tilde{\alpha}(0)e^{-(2\lambda+\mu)t} + \left[\mu(1-\lambda/\theta)/(2\lambda+\mu)\right]\left(1-e^{-(2\lambda+\mu)t}\right) \\ &\to \mu(1-\lambda/\theta)/(2\lambda+\mu) \quad \text{as } t\to\infty,\end{aligned} \tag{3.15}$$

as in (3.12).

3.4 Dose-Response for Small Steady Toxin Exposure

Of interest in risk analysis is the behavior of the dose response curve for small values of (toxic) dose. We approximate this by finding expressions for $\left.\frac{d\alpha(\tau)}{d\tau}\right|_{\tau=0}$, $\left.\frac{d\gamma(\tau)}{d\tau}\right|_{\tau=0}$, and $\left.\frac{d\beta(\tau)}{d\tau}\right|_{\tau=0}$.

Suppose $\tau(t) = \tau = \tau \sim 0$, a constant, and that exposure has proceeded for some time so that a steady-state condition has been reached; this is modeled by letting $\frac{d\alpha(t)}{dt} = \frac{d\gamma(t)}{dt} = \frac{d\beta}{dt} = 0$ in (3.8) – (3.10). To study the dose-response for $\tau \approx 0$, differentiate (3.10) with respect to τ using the function δ in (3.5) (drop subscript "o" for convenience)

$$0 = 1 - \frac{d\nu}{d\beta}\frac{d\beta}{d\tau}\frac{\alpha\beta}{1+\kappa\beta} - \frac{\nu d\alpha}{d\tau}\frac{\beta}{1+\kappa\beta} - \frac{\nu\alpha}{1+\kappa\beta}\frac{d\beta}{d\tau} + \frac{\nu\alpha\beta}{(1+\kappa\beta)^2}\frac{d\beta}{d\tau}. \tag{3.16}$$

Since $\beta = 0$ for $\tau = 0$, equation (3.6) yields for the (scaled) rate of toxin concentration at low exposure

$$\beta_\tau \equiv \left.\frac{\partial\beta}{\partial\tau}\right|_{\tau=0} = \left.\frac{1}{\nu\alpha}\right|_{\tau=0} = \frac{1}{\nu}\frac{2\lambda+\mu}{\mu\left(1-\frac{\lambda}{\theta}\right)} > 0 \quad \text{if } \frac{\lambda}{\theta} < 1. \tag{3.17}$$

This shows explicitly how low-dose toxin level in the organ tissue increases as a function of cell-cycle parameters λ and μ, signaling efficiency, θ, and toxin

metabolic or binding rate ν. All of these parameters are evaluated at very low (zero) toxin levels.

Next consider steady-state rate of change of scaled functional cell fraction, $\frac{\partial \alpha}{\partial \tau} \equiv \alpha_\tau = \alpha_\beta \cdot \beta_\tau$; this is the slope of a dose-(functioning cell count) response curve at very low levels of toxin. If (3.12) is differentiated and some rearrangements made, and if $\gamma = \lambda/\theta$ as in (3.11), then

$$\alpha_\beta = \left[-\lambda_\beta \mu(2+\lambda/\mu+2(1-\gamma)) + \mu_\beta(2\lambda(1-\gamma)) + \theta_\beta(2\lambda+\mu)(\mu/\theta)\gamma\right]\frac{1}{(2\lambda+\mu)^2}. \quad (3.18)$$

Since $\beta_\tau > 0$, the sign of α_τ is determined by the above linear combination of the derivatives of the cell cycle and signaling parameters λ, μ, and θ at τ, and hence β, equal to zero. Note that if the illustrative relations (3.4) are invoked as given, then $\alpha_\beta < 0$, hence $\alpha_\tau < 0$ so a small increase in toxin induces a decline in the number of functioning cells; this is intuitively acceptable. However, a change in sign of any of the parameters' derivatives is capable of reversing the sign of the slope of the dose response curve, thus representing a tendency for hormesis at low dose.

4. Models with Cell Aging

In this section we generalize the models of the last section to allow cells to age, and hence exist in possibly different stages of functional effectiveness.

We restrict attention to just two age stages, which we term *new* (n) and *old* (o), distinguishing them by subscript. An arbitrary number of such age states can be introduced, but at the cost of increasing the number of parameters.

Let $D_n(t)$ (respectively $D_o(t)$) represent the number of new (respectively old) cells at time t. $M(t)$ represents the number of dividing (mitotic) cells at time t and $G(t)$ the number of ambient signals or ghosts as before. The spatial constraint is

$$C_0 = D_n(t) + D_o(t) + G(t) + 2M(t). \tag{4.1}$$

Here are the transition probabilities assumed:

Signaling Model with Age Dependence
(Markov Generator)

t		$t + dt$	*Probability*
$D_n(t), D_o(t),$ $G(t), M(t);$ $T(t)$	$\rightarrow$	$D_n(t) - 1, D_o(t), G(t) + 1, M(t)$ $T(t) + \delta^* dt + \sigma dW(t)$ (new cell death, signal creation)	$\lambda_n^* D_n(t) dt$
	$\rightarrow$	$D_n(t), D_o(t) - 1, G(t) + 1, M(t)$ $T(t) + \delta^* dt + \sigma dW(t)$ (old cell death, signal creation)1	$\lambda_o^* D_o(t) dt$
	$\rightarrow$	$D_n(t) - 1, D_o(t), G(t) - 1, M(t) + 1$ $T(t) + \delta^* dt + \sigma dW(t)$ (new cell signaled to divide, signal disappears)	$\theta_n^* G(t)(D_n(t)/C_0) dt$
	$\rightarrow$	$D_n(t), D_o(t) - 1, G(t) - 1, M(t) + 1$ $T(t) + \delta^* dt + \sigma dW(t)$ (old cell signaled to divide, signal disappears)	$\theta_o^* G(t)(D_o(t)/C_0) dt$
	$\rightarrow$	$D_n(t) + 2, D_o(t), G(t), M(t) - 1$ $T(t) + \delta^* dt + \sigma dW(t)$ (two newly-divided new cells emerge)	$\mu^* M(t)\, dt$
	$\rightarrow$	$D_n(t) - 1, D_o(t) + 1, G(t), M(t)$ $T(t) + \delta^* dt + \sigma dW(t)$ (a new cell becomes an old cell)	$\phi^* D_n(t)\, dt$

(4.2)

Once again all rates of cell transition, namely λ_n^*, λ_o^*, θ_n^*, θ_o^*, μ^* are presumed to be influenced by current toxin concentration. In turn, the latter is influenced by

the metabolic capability of the cells to remove toxin, $\delta^*(T(t), D_n(t), D_o(t), \tau(t))$. When specific functions are required, we shall use for illustration

$$\delta^*(T(t),D_n(t),D_o(t),\tau(t)) = \tau^*(t) - \nu_n^* \frac{T(t)D_n(t)/C_0}{1+\kappa_n^* T(t)} - \nu_o^* \frac{T(t)D_o(t)/C_0}{1+\kappa_o^* T(t)} \quad (4.3a)$$

$$\lambda_n^*(T(t)) = \lambda_{n,0}\left(p\left(e^{\lambda_{n,1}^* T(t)} - 1\right)^+ + q\right), \qquad p+q=1,\ p \geq 0 \quad (4.3b)$$

$$\lambda_o^*(T(t)) = \lambda_{o,0}\, e^{\lambda_{o,1}^* T(t)} \quad (4.3c)$$

$$\phi^*(T(t)) = \phi_0\, e^{\phi_1^* T(t)} \quad (4.3d)$$

$$\mu^*(T(t)) = \mu_0\, e^{-\mu_1^* T(t)} \quad (4.3e)$$

The form of (4.3b) permits the adjustment of organ toxin concentration-caused cell death rate to be flexibly adjusted; if $\lambda_{n,1}^* < 0$ the inner bracket must have its sign reversed: ( )$^+$. As before, the above forms are hypothetical.

4.1 Differential Equations for Deterministic Approximations

Let C_0 denote the number of spaces/holes that cells may occupy. Then

$$C_0 = D_n(t) + D_o(t) + G(t) + 2M(t).$$

Assume that

$$\frac{D_n(t)}{C_0} \to \alpha_n(t),\ \frac{D_o(t)}{C_0} \to \alpha_o(t),\ \frac{G(t)}{C_0} \to \gamma(t),\ \frac{T(t)}{C_0} \to \beta(t) \quad (4.4)$$

in probability as $C_0 \to \infty$. The following differential equations result from direct manipulation of (4.2) with scaled rate functions

$$\frac{d\alpha_n(t)}{dt} = -\left[\lambda_n + \phi\right]\alpha_n(t) - \theta_n \alpha_n(t)\gamma(t) + \mu\left[1 - \alpha_n(t) - \alpha_o(t) - \gamma(t)\right] \quad (4.5)$$

$$\frac{d\alpha_o(t)}{dt} = -\lambda_o \alpha_o(t) + \phi\alpha_n(t) - \theta_o \alpha_o(t)\gamma(t) \quad (4.6)$$

$$\frac{d\gamma(t)}{dt} = -[\theta_n\alpha_n(t) + \theta_o\alpha_o(t)]\gamma(t) + \lambda_n\alpha_n(t) + \lambda_o\alpha_o(t) \tag{4.7}$$

$$\frac{d\beta(t)}{dt} = \tau(t) - \nu_n\alpha_n(t)\frac{\beta(t)}{1+\kappa_n\beta(t)} - \nu_o\alpha_o(t)\frac{\beta(t)}{1+\kappa_o\beta(t)} \tag{4.8}$$

These equations can be solved numerically, but not in closed parametric form.

4.2 Solution Without Toxin Input

Suppose no toxin input exists so $T(t) = 0$, $t \geq 0$. Then a steady-state solution to (4.5) – (4.7) may occur; set derivatives equal to 0 obtaining the following equations.

$$0 = -(\lambda_n + \phi)\alpha_n - \theta_n\alpha_n\gamma + \mu[1 - \alpha_n - \alpha_o - \gamma] \tag{4.9}$$

$$0 = -\lambda_o\alpha_o + \phi\alpha_n - \theta_o\alpha_o\gamma \tag{4.10}$$

$$0 = [-\theta_n\alpha_n - \theta_o\alpha_o]\gamma + \lambda_n\alpha_n + \lambda_o\alpha_o. \tag{4.11}$$

Equation (4.10) yields

$$\alpha_n = (1/\phi)[\lambda_o + \theta_o\gamma]\alpha_o. \tag{4.12}$$

Substituting (4.12) into equation (4.11) yields

$$0 = \left[-\theta_n(1/\phi)[\lambda_o + \theta_o\gamma] - \theta_o\right]\gamma + \left(\lambda_n\left[(1/\phi)[\lambda_o + \theta_o\gamma]\right] + \lambda_o\right) \tag{4.13}$$

after dividing through by α_o.

Rewriting (4.13) we obtain

$$0 = (-\theta_n\theta_o/\phi)\gamma^2 - \gamma\left[\theta_n(1/\phi)\lambda_o + \theta_o - \lambda_n(1/\phi)\theta_o\right] + \left[(\lambda_n/\phi) + 1\right]\lambda_o. \tag{4.14}$$

Thus γ satisfies a quadratic equation. Let γ_o be the positive solution to the equation. If $\lambda_n(0) = 0$, as in (4.3b)

$$\gamma_o = \frac{-\left[\frac{\lambda_o}{\theta_o} + \frac{\phi}{\theta_n}\right] + \sqrt{\left(\frac{\lambda_o}{\theta_o} + \frac{\phi}{\theta_n}\right)^2 + 4\frac{\lambda_o}{\theta_o}\frac{\phi}{\theta_n}}}{2}. \tag{4.15}$$

If $\gamma_0 < 1$, then $\gamma = \gamma_0$. If $\gamma_0 \geq 1$ then ambient signals and not functional cells dominate the organ, which in reality would be long defunct even without toxin.

If $\frac{\theta_n}{\phi} < 1$ and

$$\frac{\lambda_0}{\theta_0} < \left[1 + \frac{\theta_n}{\phi}\right] \Big/ \left[1 - \frac{\theta_n}{\phi}\right] \tag{4.16}$$

then $\gamma_0 < 1$.

To find α_0 equation (4.9) is used. Put $c_1 = (1/\phi)[\lambda_0 + \theta_0\gamma]$. Then

$$\mu[1-\gamma_0] = \{(\lambda_n + \phi)c_1 + \theta_n\gamma c_1 + \mu[c_1 + 1]\}\alpha_0 = \{2\lambda_0 + \mu[c_1 + 1] + 2\lambda_n c_1\}\alpha_0.$$

Thus,

$$\alpha_0 = \mu[1-\gamma_0] / \{2\lambda_0 + \mu[1 + c_1] + 2\lambda_n c_1\} \tag{4.17}$$

and

$$\alpha_n = c_1\alpha_0. \tag{4.18}$$

4.3 Dose-Response For Small Steady Toxin Input

As mentioned earlier, the behavior of an organ-level dose-response curve for small values of toxic dose is of interest in risk analysis. In this section we indicate that the derivative of various cellular-level responses with respect to τ may be evaluated at $\tau = 0$.

If $\tau = 0$ then $\beta = 0$. Set the left-hand side of (4.8) equal to zero, then differentiate the right side with respect to τ. After setting $\beta = 0$, this yields

$$0 = 1 - [\nu_n\alpha_n + \nu_0\alpha_0]\frac{d\beta}{d\tau}. \tag{4.19}$$

Thus

$$\left.\frac{d\beta}{d\tau}\right|\tau = 0 = \frac{1}{\nu_n\alpha_n + \nu_0\alpha_0} > 0, \tag{4.20}$$

as is physically plausible.

It may be shown by further differentiation that under the specific parameterization of (3.4), or suitable alternatives, all derivatives of long-run cellular-level response can be explicitly evaluated at $\tau = 0$, as was shown earlier. The complex details are omitted here.

5. A Model with Cell Aging and Organ Tissue Growth

In this section we generalize the previous model to allow cells to spontaneously enter mitosis and multiply, thus effectively increasing the organ size, where the latter is defined as the number of cells in existence, in either state. In the previous section cell replication only occurred to replace other cells that previously have died, possibly as a result of toxin action.

Consider the region to be occupied by cells to consist of spaces/holes that may be filled by cells. Let C_0 be the maximum number of such holes, in this case the number in an essentially mature organ. Initially not all such holes are *active*, for the organ is immature and hence growing. Hence let $C(t)$ be the number of active holes at time t, while $C_0 - C(t)$ are currently quiescent or inactive. Now, generalizing the previous setup, let the current number of active holes/spaces be

$$C(t) = D_n(t) + D_0(t) + G(t) + 2M(t) \tag{5.1}$$

and augment the previous model to allow $C(t)$ to gradually grow, although remaining bounded by C_0.

5.1 Organ Growth Stimulated by Signaling

In this model the presence of inactive holes/spaces effectively encourages the active cells, $D_n(t)$ and $D_0(t)$, to increase the number of signals and hence the number of active spaces capable of accomodating cells. We are implicitly modeling the competing effects of positive and negative, or inhibitory, growth factors.

The model is specified by the following transitions.

Signaling-Driven Organ Growth
(Markov Generator)

t	$t+dt$	*Probability*	
$D_n(t), D_0(t),$ $G(t), M(t),$ $C(t)\ T(t)$	$\rightarrow$ $D_n(t), D_0(t), G(t)+1, M(t), C(t)+1$ $T(t)+\delta dt+\sigma dW(t)$ (a quiescent cell space becomes active, signal creation)	$\left[\xi_n^* D_n(t)+\xi_0^* D_0(t)\right]\left[1-\frac{C(t)}{C_0}\right]dt$	
	$\rightarrow$ $D_n(t)-1, D_0(t), G(t)+1, M(t), C(t)$ $T(t)+\delta dt+\sigma dW(t)$ (new cell death, signal creation)	$\lambda_n^* D_n(t)dt$	
	$\rightarrow$ $D_n(t), D_0(t)-1, G(t)+1, M(t), C(t)$ $T(t)+\delta dt+\sigma dW(t)$ (old cell death, signal creation)	$\lambda_0^* D_0(t)dt$	
	$\rightarrow$ $D_n(t)+2, D_0(t), G(t)+1, M(t)-1, C(t)$ $T(t)+\delta dt+\sigma dW(t)$ (two newly-divided cells emerge)	$\mu^* M(t)dt$	(5.2)
	$\rightarrow$ $D_n(t)-1, D_0(t)+1, G(t), M(t), C(t)$ $T(t)+\delta dt+\sigma dW(t)$ (new cell becomes old)	$\phi^* D_n(t)dt$	
	$\rightarrow$ $D_n(t)-1, D_0(t), G(t)-1, M(t)+1, C(t)$ $T(t)+\delta dt+\sigma dW(t)$ (new cell signaled to divide, signal vanishes)	$\theta_n^* G(t)\frac{D_n(t)}{C(t)}dt$	
	$\rightarrow$ $D_n(t), D_0(t)-1, G(t)-1, M(t)+1, C(t)$ $T(t)+\delta dt+\sigma dW(t)$ (old cell signaled to divide, signal vanishes)	$\theta_0^* G(t)\frac{D_0(t)}{C(t)}dt$	

Once again, all rates of cell transition, namely, λ_n^*, λ_o^*, θ^*, ϕ^*, μ^*, ξ_n^*, ξ_o^* are presumed to be influenced by current toxin concentration. When specific functions are required we shall use

$$\begin{aligned} \xi_n^*(T(t)) &= \xi_{n,0} e^{-\xi_{n,1}^* T(t)} \\ \xi_n^*(T(t)) &= \xi_{o,0} e^{-\xi_{o,1}^* T(t)} \end{aligned} \tag{5.3}$$

in addition to those of (4.3 a–e).

Once again assume that as $C_0 \to \infty$

$$\frac{D_n(t)}{C_0} \to \alpha_n(t),\ \frac{D_o(t)}{C_0} \to \alpha_o(t),\ \frac{G(t)}{C_0} \to \gamma(t),\ \frac{C(t)}{C_0} \to \eta(t),\ \frac{T(t)}{C_0} \to \beta(t) \tag{5.4}$$

in probability.

The following differential equations result from direct manipulation of (5.2).

$$\frac{d\alpha_n(t)}{dt} = -\left[\lambda_n + \phi\right]\alpha_n(t) - \theta_n \frac{\alpha_n(t)}{\eta(t)}\gamma(t) + \mu(\eta(t) - \alpha_n(t) - \alpha_o(t) - \gamma(t)) \tag{5.5}$$

$$\frac{d\alpha_o(t)}{dt} = -\lambda_o \alpha_o(t) - \theta_o \frac{\alpha_o(t)}{\eta(t)}\gamma(t) + \phi\alpha_n(t) \tag{5.6}$$

$$\frac{d\gamma(t)}{dt} = -\frac{\left[\theta_n \alpha_n(t) + \theta_o \alpha_o(t)\right]}{\eta(t)}\gamma(t) + \lambda_n \alpha_n(t) + \lambda_o \alpha_o(t) + \left[\xi_o \alpha_o(t) + \xi_n \alpha_n(t)\right]\left[1 - \eta(t)\right] \tag{5.7}$$

$$\frac{d\eta(t)}{dt} = \left[\xi_n \alpha_n(t) + \xi_o \alpha_o(t)\right]\left[1 - \eta(t)\right] \tag{5.8}$$

$$\frac{d\beta(t)}{dt} = \delta \tag{5.9}$$

6. Stochastic Differential Equation Models

The size of the state space makes the time-dependent behavior of the continuous-time Markov chain models of Sections 3 – 5 difficult to study. One

approach to studying the behavior is by Monte Carlo simulation; cf. Bois, et al. (1992). Another approach, adopted here, is to approximate the continuous-time Markov chain model by a diffusion process. Note that the continuous-time Markov chain model has absorbing states; for example, any state with $D_n(t) + D_o(t) = 0$ is absorbing. Of course no self-respecting organ would ever start life in such a state, and a living organ would presumably die from other unmodeled causes long before such a state is reached, i.e. when $D_n(t) + D_o(t) \le D$, some lower limit. Barbour (1976) discusses how long and over what ranges the underlying continuous-time Markov chain is approximated by a diffusion process of the type we derive; see also discussion to McNeil and Schach (1973). Stochastic differential equation models can be written for all the models of Sections 3 – 5. We will illustrate our approach by writing down a system of stochastic differential equations for the multivariate process $(D_n(t), D_o(t), G(t), C(t), T(t))$ for Markov generator (5.2). The system of stochastic differential equations is as follows; as explained subsequently, the dW-terms are normally distributed.

$$\left.\begin{aligned} dD_n(t) = {} & -\lambda_n^*(T(t))D_n(t)dt - \theta_n^*(T(t))G(t)(D_n(t)/C(t))dt \\ & -\phi^*(T(t))D_n(t)dt + \mu^*(T(t))(C(t) - D_n(t) - D_o(t) - G(t))dt \end{aligned}\right\} \begin{pmatrix}\text{drift = conditional}\\ \text{expected change}\\ \text{in } (t, t+dt)\end{pmatrix}$$

$$\left.\begin{aligned} & -\sqrt{\varepsilon\lambda_n^*(T(t))D_n(t)}\,dW_{\lambda_n}(t) - \sqrt{\varepsilon\phi^*(T(t))D_n(t)}\,dW_{\phi}(t) \\ & -\sqrt{\varepsilon\theta_n^*(T(t))G(t)(D_n(t)/C(t))}\,dW_{\theta_n}(t) \\ & +\sqrt{\varepsilon 4\mu^*(T(t))(C(t) - D_n(t) - D_o(t) - G(t))\frac{1}{2}}\,dW_{\mu}(t) \end{aligned}\right\} \begin{pmatrix}\text{diffusion = random}\\ \text{change in } (t, t+dt)\end{pmatrix} \qquad (6.1)$$

$$
\begin{aligned}
dD_o(t) = &-\lambda_o^*(T(t))D_o(t)dt - \theta_o^*(T(t))G(t)(D_o(t)/C(t))dt \\
&+\phi^*(T(t))D_n(t)dt \qquad \text{(drift)} \\
&-\sqrt{\varepsilon\lambda_o^*(T(t))D_o(t)}\,dW_{\lambda_o}(t) + \sqrt{\varepsilon\phi^*(T(t))D_n(t)}\,dW_{\phi}(t) \\
&-\sqrt{\varepsilon\theta_o^*(T(t))G(t)(D_o(t)/C(t))}\,dW_{\theta_o}(t) \qquad \text{(diffusion)}
\end{aligned}
\tag{6.2}
$$

$$
\begin{aligned}
dG(t) = &-\theta_n^*(T(t))G(t)(D_n(t)/C(t))dt - \theta_o^*(T(t))G(t)(D_o(t)/C(t))dt \\
&+\lambda_o^*(T(t))D_o(t)dt + \lambda_n^*(T(t))D_n(t)dt \\
&+\xi_n^*(T(t))D_n(t)\left[1-\frac{C(t)}{C_0}\right] + \xi_o^*(T(t))D_o(t)\left[1-\frac{C(t)}{C_0}\right] \qquad \text{(drift)} \\
&-\sqrt{\varepsilon\theta_n^*(T(t))G(t)(D_n(t)/C(t))}\,dW_{\theta_n}(t) \\
&-\sqrt{\varepsilon\theta_o^*(T(t))G(t)(D_o(t)/C(t))}\,dW_{\theta_o}(t) \\
&+\sqrt{\varepsilon\lambda_o^*(T(t))D_o(t)}\,dW_{\lambda_o}(t) + \sqrt{\varepsilon\lambda_n^*(T(t))D_n(t)}\,dW_{\lambda_n}(t) \\
&+\sqrt{\varepsilon\xi_n^*(T(t))D_n(t)\left[1-\frac{C(t)}{C_0}\right]}\,dW_{\xi_n}(t) \\
&+\sqrt{\varepsilon\xi_o^*(T(t))D_o(t)\left[1-\frac{C(t)}{C_0}\right]}\,dW_{\xi_o}(t) \qquad \text{(diffusion)}
\end{aligned}
\tag{6.3}
$$

$$\frac{dC(t)}{dt} = \xi_o^*(T(t))D_o(t)\left[1-\frac{C(t)}{C_0}\right] + \xi_n^*(T(t))D_n(t)\left[1-\frac{C(t)}{C_0}\right]\Big\}\text{(drift)}$$

$$\left.\begin{aligned} &+\sqrt{\varepsilon\xi_o^*(T(t))D_o(t)\left[1-\frac{C(t)}{C_0}\right]}\,dW_{\xi_o}(t) \\ &+\sqrt{\varepsilon\xi_n^*(T(t))D_n(t)\left[1-\frac{C(t)}{C_0}\right]}\,dW_{\xi_n}(t) \end{aligned}\right\}\text{(diffusion)} \qquad (6.4)$$

$$\frac{dT(t)}{dt} = \delta^*\left(T(t), D_n(t), D_o(t), \tau^*(t)\right)dt\Big\}\text{(drift)}$$

$$\left.\begin{aligned} &+\sigma_T^*(T(t), D_n(t), D_o(t), \tau(t))dW_{\sigma_T}(t) \\ &+\sqrt{C_0}\sigma_\tau dW_\tau(t) \end{aligned}\right\}\text{(diffusion)} \qquad (6.5)$$

where $\{W_{\lambda_n}(t)\}, \{W_{\lambda_o}(t)\}, \{W_{\theta_n}(t)\}, \{W_{\theta_o}(t)\}, \{W_\mu(t)\}, \{W_{\xi_o}(t)\}, \{W_{\xi_n}(t)\}, \{W_{\sigma_T}(t)\}$, and $\{W_\tau(t)\}$ are independent standard Brownian motions; each $dW(t)$-term is thus Gaussian with mean zero and variance dt.

Setting the constant $\varepsilon = 1$ lets the variances of the change in the number of active cells, ghosts in identified states, and active spaces be equal to the mean respective changes; this represents Poisson variability. Setting the constant $\varepsilon > 1$ implies that the variability is larger than Poisson variability. This additional variability may be the result of inhomogeneities in the organ that are not explicitly modeled; cf. Bass, Robinson and Bracken (1978) for discussion of a distributed liver model with random inhomogeneities. Such *overdispersion* is frequently encountered in practice, and may be accounted for parsimoniously as we do; see McCullagh and Nelder (1983).

We assume that as $C_0 \to \infty$

$$\frac{D_n(t)}{C_0} \to \alpha_n(t),\ \frac{D_o(t)}{C_0} \to \alpha_o(t),\ \frac{G(t)}{C_0} \to \gamma(t),\ \frac{C(t)}{C_0} \to \eta(t),\ \frac{T(t)}{C_0} \to \beta(t) \qquad (6.6)$$

in probability and rewrite $D_n(t)$, $D_o(t)$, $G(t)$, $C(t)$, and $T(t)$ as follows.

$$D_n(t) = C_0\alpha_n(t) + \sqrt{C_0}X_n(t) \tag{6.7a}$$

$$D_o(t) = C_0\alpha_o(t) + \sqrt{C_0}X_o(t) \tag{6.7b}$$

$$G(t) = C_0\gamma(t) + \sqrt{C_0}X_g(t) \tag{6.7c}$$

$$C(t) = C_0\eta(t) + \sqrt{C_0}X_c(t) \tag{6.7d}$$

$$T(t) = C_0\beta(t) + \sqrt{C_0}Y(t) \tag{6.7e}$$

$$d\tau^*(t) = C_0\tau(t) + \sqrt{C_0}\sigma_\tau dW_\tau(t) \tag{6.7f}$$

The transition rates will be scaled and expanded as follows:

$$\lambda_n^*(T(t)) = \lambda_n(T(t)/C_0) = \lambda_n(\beta(t)) + \lambda_n'(\beta(t))Y(t)/\sqrt{C_0} + O(1) \tag{6.8a}$$

$$\lambda_o^*(T(t)) = \lambda_o(T(t)/C_0) = \lambda_o(\beta(t)) + \lambda_o'(\beta(t))Y(t)/\sqrt{C_0} + O(1) \tag{6.8b}$$

$$\mu^*(T(t)) = \mu(T(t)/C_0) = \mu(\beta(t)) + \mu'(\beta(t))Y(t)/\sqrt{C_0} + O(1) \tag{6.8c}$$

$$\theta_n^*(T(t)) = \theta_n(T(t)/C_0) = \theta_n(\beta(t)) + \theta_n'(\beta(t))Y(t)/\sqrt{C_0} + O(1) \tag{6.8d}$$

$$\theta_o^*(T(t)) = \theta_o(T(t)/C_0) = \theta_o(\beta(t)) + \theta_o'(\beta(t))Y(t)/\sqrt{C_0} + O(1) \tag{6.8e}$$

$$\xi_n^*(T(t)) = \xi_n(T(t)/C_0) = \xi_n(\beta(t)) + \xi_n'(\beta(t))Y(t)/\sqrt{C_0} + O(1) \tag{6.8f}$$

$$\xi_o^*(T(t)) = \xi_o(T(t)/C_0) = \xi_o(\beta(t)) + \xi_o'(\beta(t))Y(t)/\sqrt{C_0} + O(1) \tag{6.8g}$$

$$\delta^*\left(D_n(t),D_o(t),T(t),\tau^*(t)\right)=C_0\delta\left(D_n(t)/C_0,D_o(t)/C_0,T(t)/C_0,\tau^*(t)/C_0\right)$$

$$=C_0\delta(\alpha_n(t),\alpha_o(t),\beta(t),\tau(t)) \tag{6.8h}$$

$$+C_0\delta'_{\alpha_n}\frac{X_n(t)}{\sqrt{C_0}}+C_0\delta'_{\alpha_o}\frac{X_o(t)}{\sqrt{C_0}}+C_0\delta'_{\beta}\frac{Y(t)}{\sqrt{C_0}}+O(1)$$

$$\sigma_T^*\left(D_n(t),D_o(t),T(t),\tau^*(t)\right)=\sqrt{C_0}\sigma_T\left(D_n(t)/C_0,D_o(t)/C_0,T(t)/C_0,\tau^*(t)/C_0\right) \tag{6.8i}$$

$$=\sqrt{C_0}\sigma_T(\alpha_n(t),\alpha_o(t),\beta(t),\tau(t))+O(1)$$

Dividing equations (6.1) – (6.5) by C_0, scaling and substituting (6.7a) – (6.7f) results in a system of equations involving the deterministic components $\alpha_n(t)$, $\alpha_o(t)$, $\gamma(t)$, $\eta(t)$, and $\beta(t)$ and the corresponding stochastic components $X_n(t)$, $X_o(t)$, $Xg(t)$, $X_c(t)$, and $Y(t)$. See Appendix 1 for details.

6.1 Second Moments

The stochastic differential equations (A.1) – (A.10) of Appendix 1, derived for the stochastic disturbances, can be written in matrix-vector form as

$$d\mathbf{Z}(t) = \mathbf{A}(t)\mathbf{Z}(t) + \mathbf{B}(t)\,d\mathbf{W}(t) \tag{6.9}$$

where in the present example $\mathbf{Z}$ is a 5×1 column vector, $\mathbf{A}$ is a 5×5 matrix, $d\mathbf{W}(t)$ is 10×1 column of independent Gaussian noise terms and $\mathbf{B}(t)$ is a 5×10 matrix.

It follows from theorem (8.5.5) of Arnold (1974) that

$$\frac{d}{dt}E\left[\mathbf{Z}_i^2(t)\right]=2\sum_j \mathbf{A}_{ij}(t)E\left[\mathbf{Z}_i(t)\mathbf{Z}_j(t)\right]+\sum_j\left(\mathbf{B}_{ij}(t)\right)^2 \tag{6.10}$$

and

$$\frac{d}{dt}E\left[\mathbf{Z}_i(t)\mathbf{Z}_j(t)\right]=\sum_k \mathbf{A}_{ik}(t)E\left[\mathbf{Z}_k(t)\mathbf{Z}_j(t)\right]$$

$$+\sum_k \mathbf{A}_{jk}(t)E\left[\mathbf{Z}_k(t)\mathbf{Z}_i(t)\right] \qquad (6.11)$$

$$+\sum_k \mathbf{B}_{ik}(t)\mathbf{B}_{jk}(t)$$

Thus, the approximate distribution of $D_n(t)$, (respectively $D_o(t)$, $G(t)$, $C(t)$, $T(t)$) is normal with mean $C_0\alpha_n(t)$, (respectively $C_0\alpha_o(t)$, $C_0\gamma(t)$ $C_0\eta(t)$, $C_0\beta(t)$) and variance $C_0E\left[X_n^2(t)\right]$, (respectively $C_0E\left[X_o^2(t)\right]$, $C_0E\left[X_g^2(t)\right]$, $C_0E\left[X_c^2(t)\right]$, $C_0E\left[Y^2(t)\right]$). The approximate covariance of $D_n(t)$ and $D_o(t)$ is $C_0E[X_n(t)X_o(t)]$, etc.

We point out that exactly equivalent results can be obtained by introducing transforms for the state variables, computed by taking conditional mathematical expectations of exponential functions of the Markov generators. This is the route followed by McNeil and Schach (1973); see also Carpenter, Gaver, and Jacobs (1993). The transform approach provides a verification that the asymptotics described here actually lead to limiting Gaussian distributions and to Ornstein-Uhlenbeck processes. See Ethier and Kurtz (1986) for a more rigorous discussion. The approach taken here, while heuristic, is intuitively appealing and reaches the same ultimate conclusion.

6.2 Numerical Examples

In this section we present three numerical examples.

a. Constant Rate of Input of Toxin

We assume chronic dosage of the organ by toxin that is delivered there at constant mean rate but with substantial randomness around that mean.

Figures 1 – 5 depict the time variation of the expected numbers of new cells, of old cells, of total number of active (new plus old) cells, number of signals

(ghosts), and amount of toxin plus/minus two population standard deviations. There is no organ growth. The initial conditions are the limiting moments with no toxin input. The toxin input rate 0.2 units/cell for all time. The new cells without toxin have mean time 100 before transitioning to old. The old cells have mean lifetime of 100 without toxin. The number of cells in the organ is 1.5×10^8. The organ size is about that of a mouse liver. Since the cells in a mouse liver have a mean lifetime of about 200 days; cf. Bois, et al. (1992), the above is consistent with mouse liver behavior. The MATLAB 4^{th} and 5^{th} order Runge-Kutta-Fehlberg numerical integration method was used to obtain the solutions. The MATLAB plotting algorithms were used to produce the figures.

There is extra Poisson variability: $\varepsilon = 10^4$.

Note that the total mean number of active (new and old) cells decreases as the result of toxin input, as seems intuitively reasonable. The mean number of new cells initially decreases, but eventually increases to a new steady-state value which is larger than the value with no toxin. The mean number of old cells initially increases briefly, but then decreases to a new steady-state value below the value for no toxin. The mean amount of toxin and the mean number of signals (ghosts) both increase to new steady-state values.

The above hypothetical example illustrates how model parametric inputs translate into an account of the dynamics of subpopulations of cells. The details of the transition from one steady-state situation to another are of possible interest in that the organ may be in jeopardy during that transitional period because of, for example, new cell initial downward fluctuation. The effect on organ mortality is, however, not explicitly modeled.

b. A Toxin Pulse or Bolus Dose

Figures 6 – 10 display the mean number of new cells, old cells, active cells (new and old), signals (ghosts) and amount of toxin plus and minus 2 standard deviations for the case in which the rate of toxin input is 0.2 per cell for the first 50 time units and 0 thereafter. Once again there is no organ growth. The initial conditions are steady-state values when there is no toxin input. Note that the number of active cells decreases during toxin input, then increases and slightly overshoots the steady-state value with no toxin before returning to its steady-state value with no toxin.

c. Organ Growth

The model of Section 5.1 and (6.1) – (6.5) is initialized with the steady-state values for the second moments with no input of toxin. However, only 1/2 of the available spaces are active (may contain cells); the steady-state mean of new and old cells and ghosts for no toxin input are multiplied by 1/2 and used as initial values. Figures 11 – 15 display the mean numbers of new, old, and active cells, ghosts, and active spaces plus/minus two standard deviations for the case of no toxin input and parameters $\xi_{n,0} = 0.5$, $\xi_{n,1} = 0.5$, $\xi_{o,0} = 1$, $\xi_{o,1} = 0.5$. The mean number of active spaces is the maximum number by time 20. However, the mean number of old and new cells is still adjusting by time 100. The mean number of old cells initially decreases before increasing. The mean number of new cells initially increases before decreasing.

The present model might be useful for describing the aftermath of a partial hepatechtomy: about one-half of a mature liver remains, and grows back with subpopulations of cells responding as shown. Note that, according to the present model in Figure 12, the organ must withstand an early signal to old cells to undergo substantial depletion to enter mitosis and bring forth replacements; the

latter are the new cells depicted in Figure 11. It may be that the sudden depletion of old cells to their low point at about $t = 6$ (Figure 12) actually puts the organ in jeopardy.

Figures 16 – 21 display the mean number of new, old, and active cells, ghosts and active spaces plus/minus two standard deviations for the same parameters as used in Figures 11 – 15 but with two levels of toxin input. The dashed lines correspond to no toxin input. The solid lines correspond to a constant toxin input of 0.2 per cell per unit time. The graphs with positive toxin input have the same general shape as those with no toxin input. The mean number of new cells is initially less for a positive toxin input than for no toxin input. However, by time 100 the mean number of new cells with positive toxin input is becoming larger than that for no toxin input.

The effect of positive toxin input on the mean number of old cells is that it is initially larger than that for no toxin but by time 100 the mean number of old cells with positive toxin is less than that for no toxin. The effect of positive toxin input on the mean number of active (old and new) cells is to decrease it and delay its approach to a steady state value. The mean number of ghosts is larger with positive toxin input. Positive toxin input delays the overall growth in the number of active spaces.

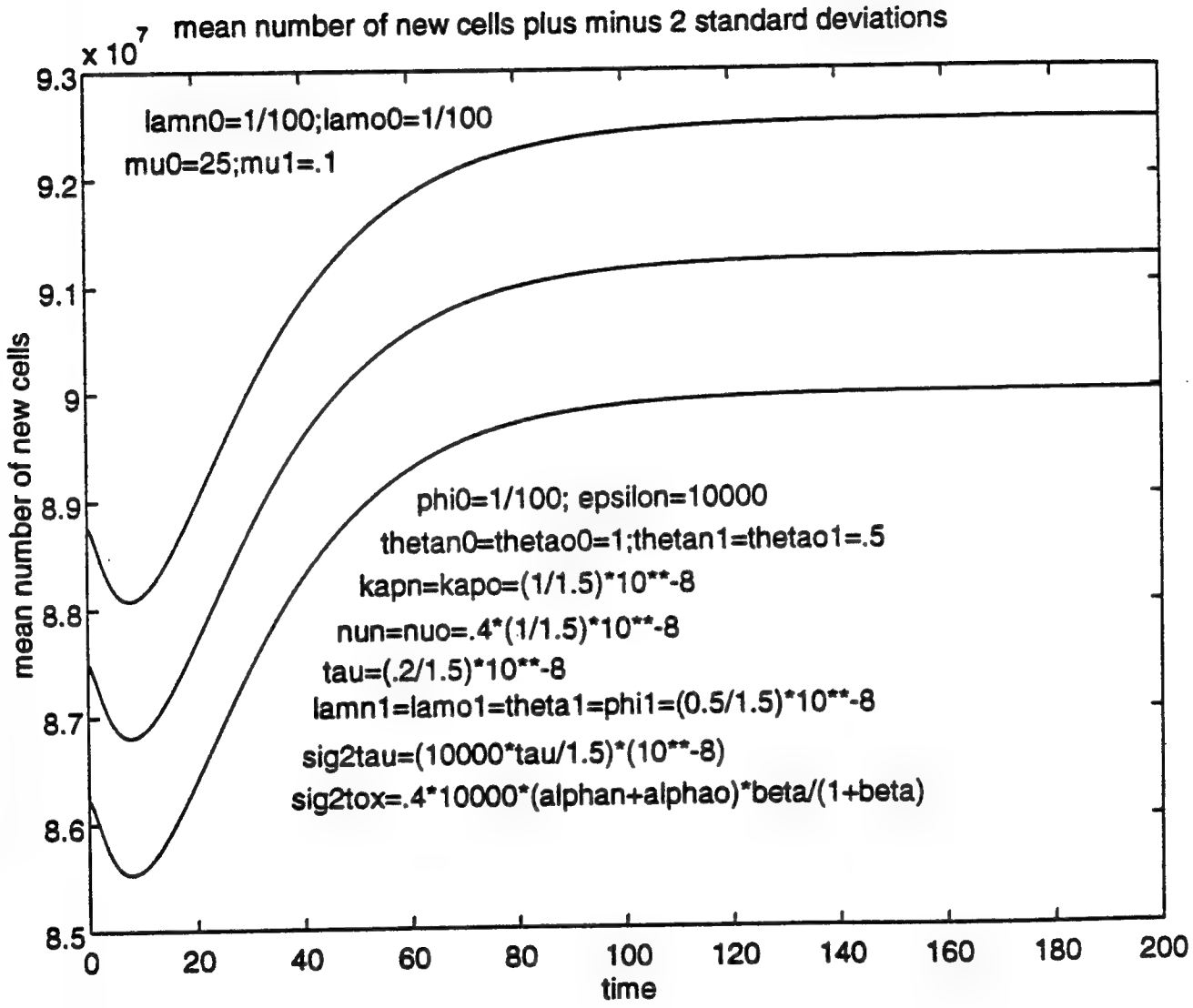
mean number of new cells plus minus 2 standard deviations
x 10^7
9.3
9.2
9.1
9
8.9
8.8
8.7
8.6
8.5
mean number of new cells
0
20
40
60
80
100
120
140
160
180
200
time
lamn0=1/100;lamo0=1/100
mu0=25;mu1=.1
phi0=1/100; epsilon=10000
thetan0=thetao0=1;thetan1=thetao1=.5
kapn=kapo=(1/1.5)*10**-8
nun=nuo=.4*(1/1.5)*10**-8
tau=(.2/1.5)*10**-8
lamn1=lamo1=theta1=phi1=(0.5/1.5)*10**-8
sig2tau=(10000*tau/1.5)*(10**-8)
sig2tox=.4*10000*(alphan+alphao)*beta/(1+beta)

Figure 1

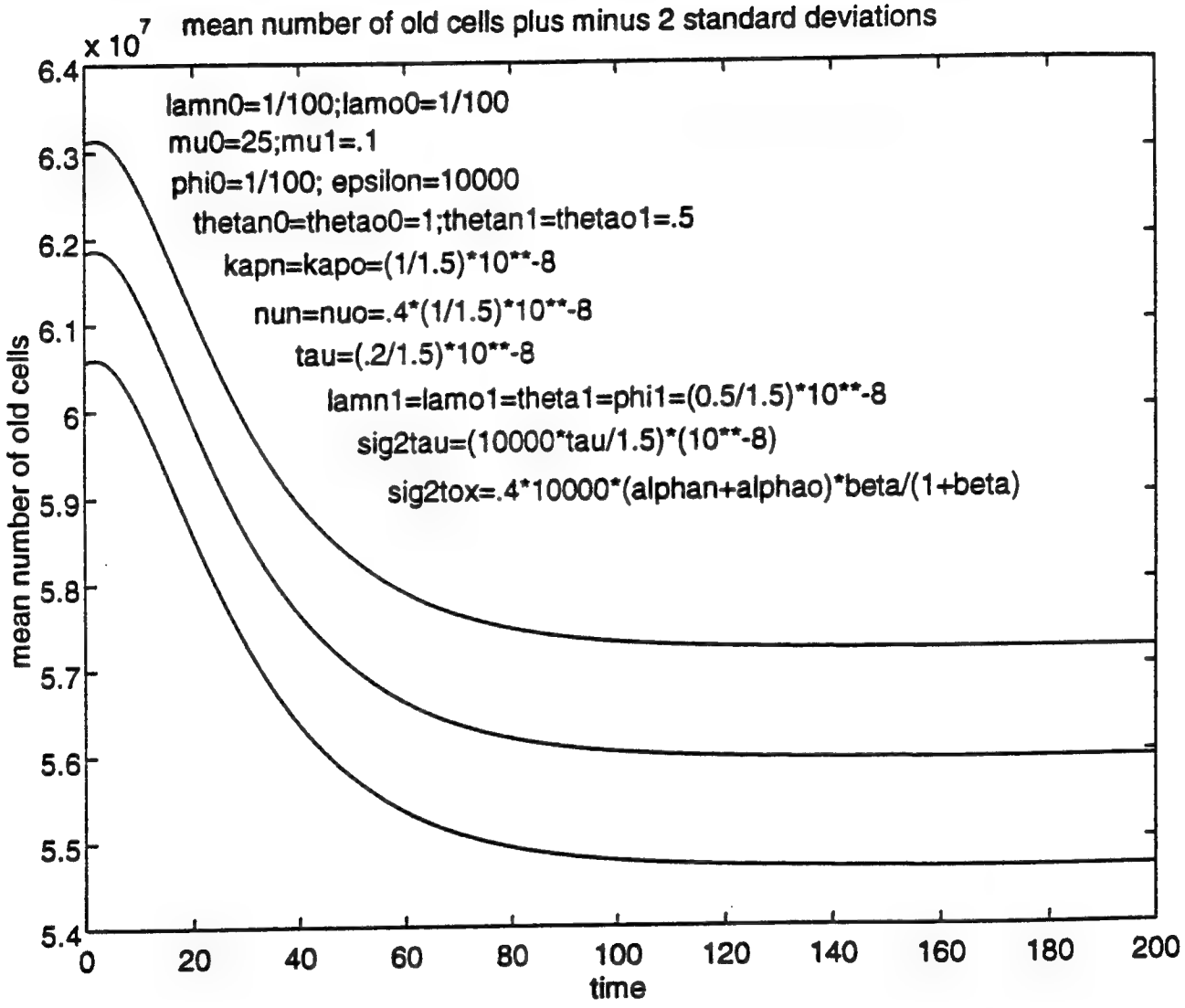
mean number of old cells plus minus 2 standard deviations
x 10^7
6.4
6.3
6.2
6.1
6
5.9
5.8
5.7
5.6
5.5
5.4
mean number of old cells
0
20
40
60
80
100
120
140
160
180
200
time
lamn0=1/100;lamo0=1/100
mu0=25;mu1=.1
phi0=1/100; epsilon=10000
thetan0=thetao0=1;thetan1=thetao1=.5
kapn=kapo=(1/1.5)*10**-8
nun=nuo=.4*(1/1.5)*10**-8
tau=(.2/1.5)*10**-8
lamn1=lamo1=theta1=phi1=(0.5/1.5)*10**-8
sig2tau=(10000*tau/1.5)*(10**-8)
sig2tox=.4*10000*(alphan+alphao)*beta/(1+beta)

Figure 2

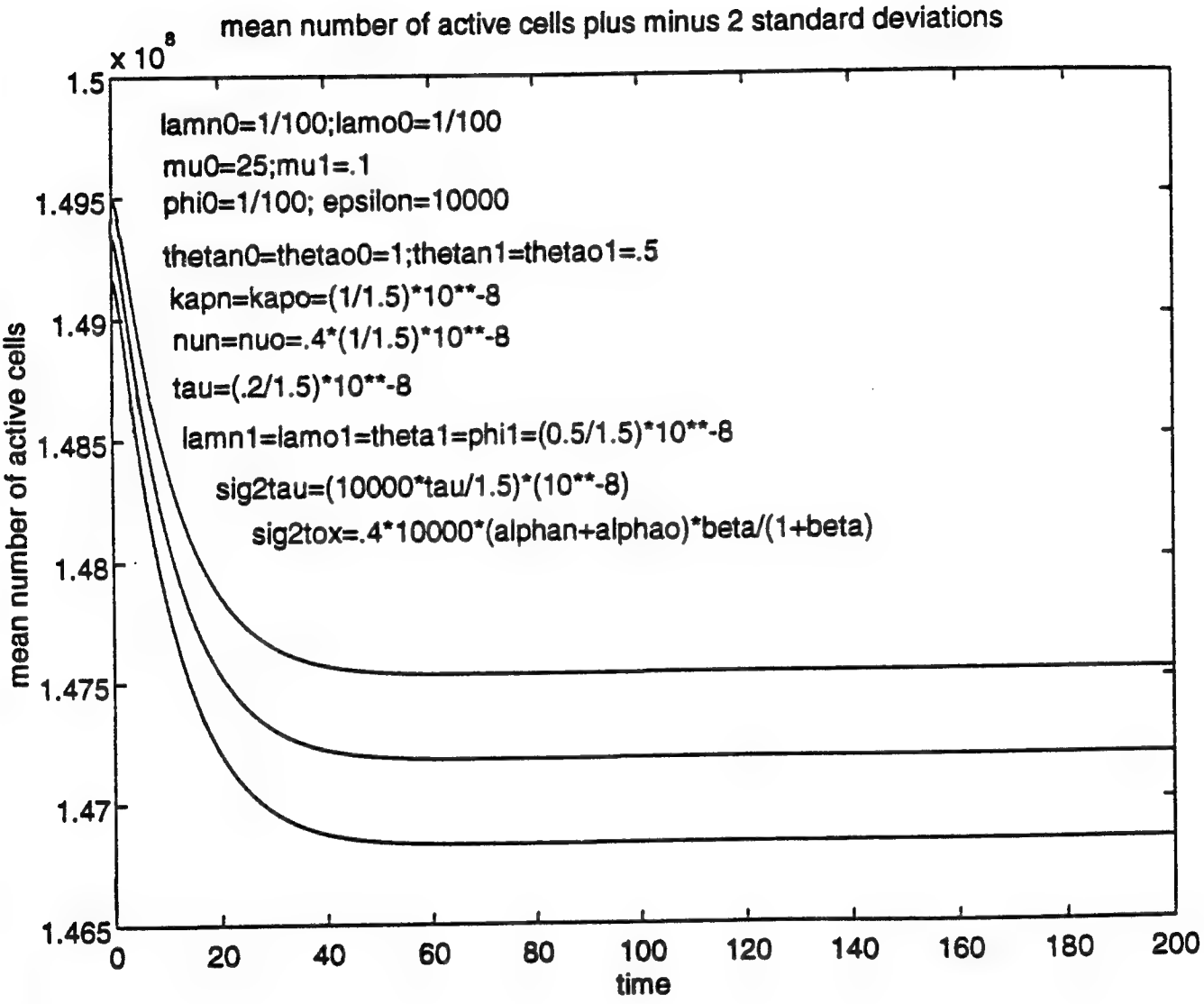
mean number of active cells plus minus 2 standard deviations
x 10^8
1.5
1.495
1.49
1.485
1.48
1.475
1.47
1.465
mean number of active cells
lamn0=1/100;lamo0=1/100
mu0=25;mu1=.1
phi0=1/100; epsilon=10000
thetan0=thetao0=1;thetan1=thetao1=.5
kapn=kapo=(1/1.5)*10**-8
nun=nuo=.4*(1/1.5)*10**-8
tau=(.2/1.5)*10**-8
lamn1=lamo1=theta1=phi1=(0.5/1.5)*10**-8
sig2tau=(10000*tau/1.5)*(10**-8)
sig2tox=.4*10000*(alphan+alphao)*beta/(1+beta)
0
20
40
60
80
100
120
140
160
180
200
time

Figure 3

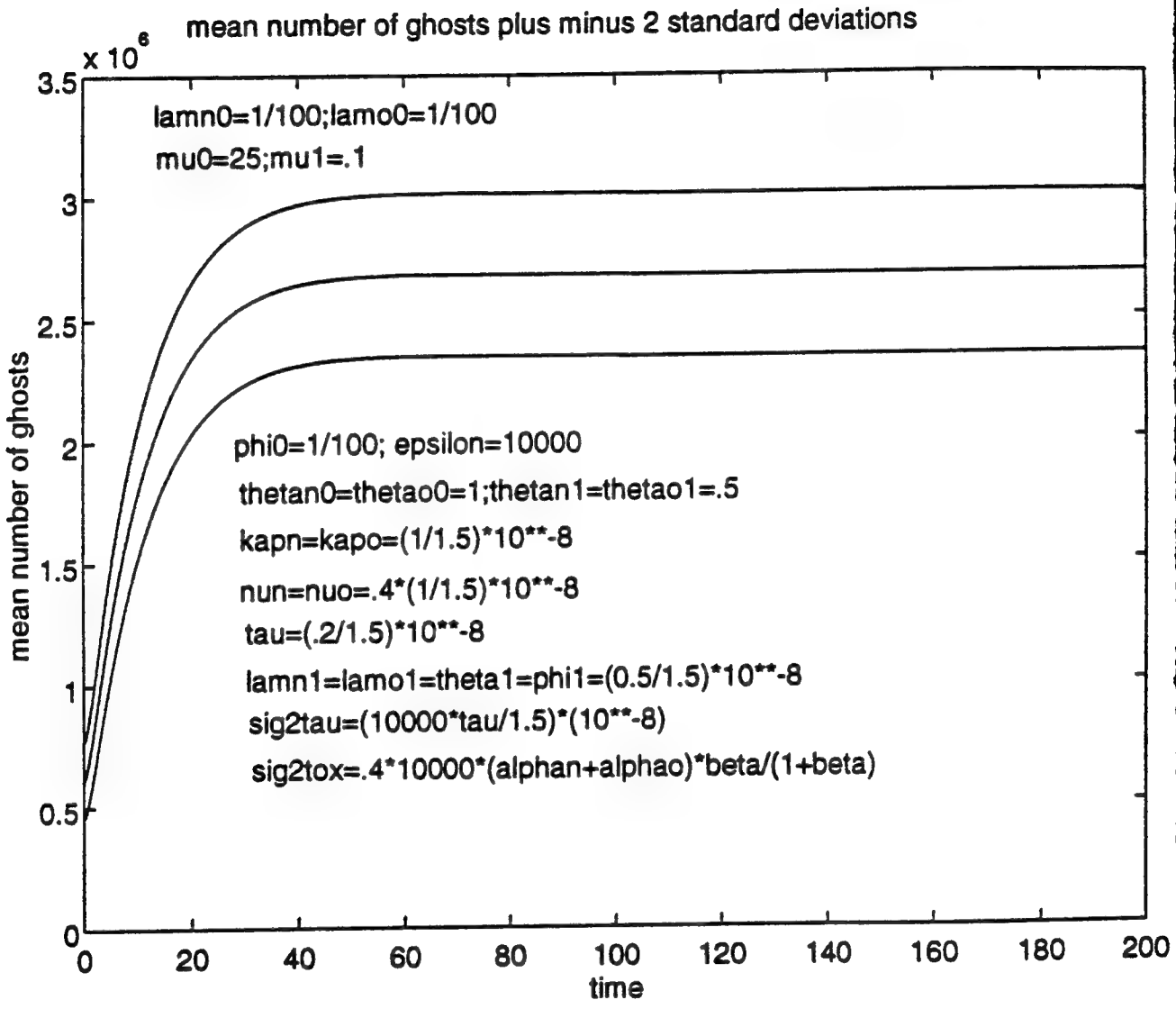
mean number of ghosts plus minus 2 standard deviations
x 10^6
3.5
3
2.5
2
1.5
1
0.5
0
mean number of ghosts
lamn0=1/100;lamo0=1/100
mu0=25;mu1=.1
phi0=1/100; epsilon=10000
thetan0=thetao0=1;thetan1=thetao1=.5
kapn=kapo=(1/1.5)*10**-8
nun=nuo=.4*(1/1.5)*10**-8
tau=(.2/1.5)*10**-8
lamn1=lamo1=theta1=phi1=(0.5/1.5)*10**-8
sig2tau=(10000*tau/1.5)*(10**-8)
sig2tox=.4*10000*(alphan+alphao)*beta/(1+beta)
0
20
40
60
80
100
120
140
160
180
200
time

Figure 4

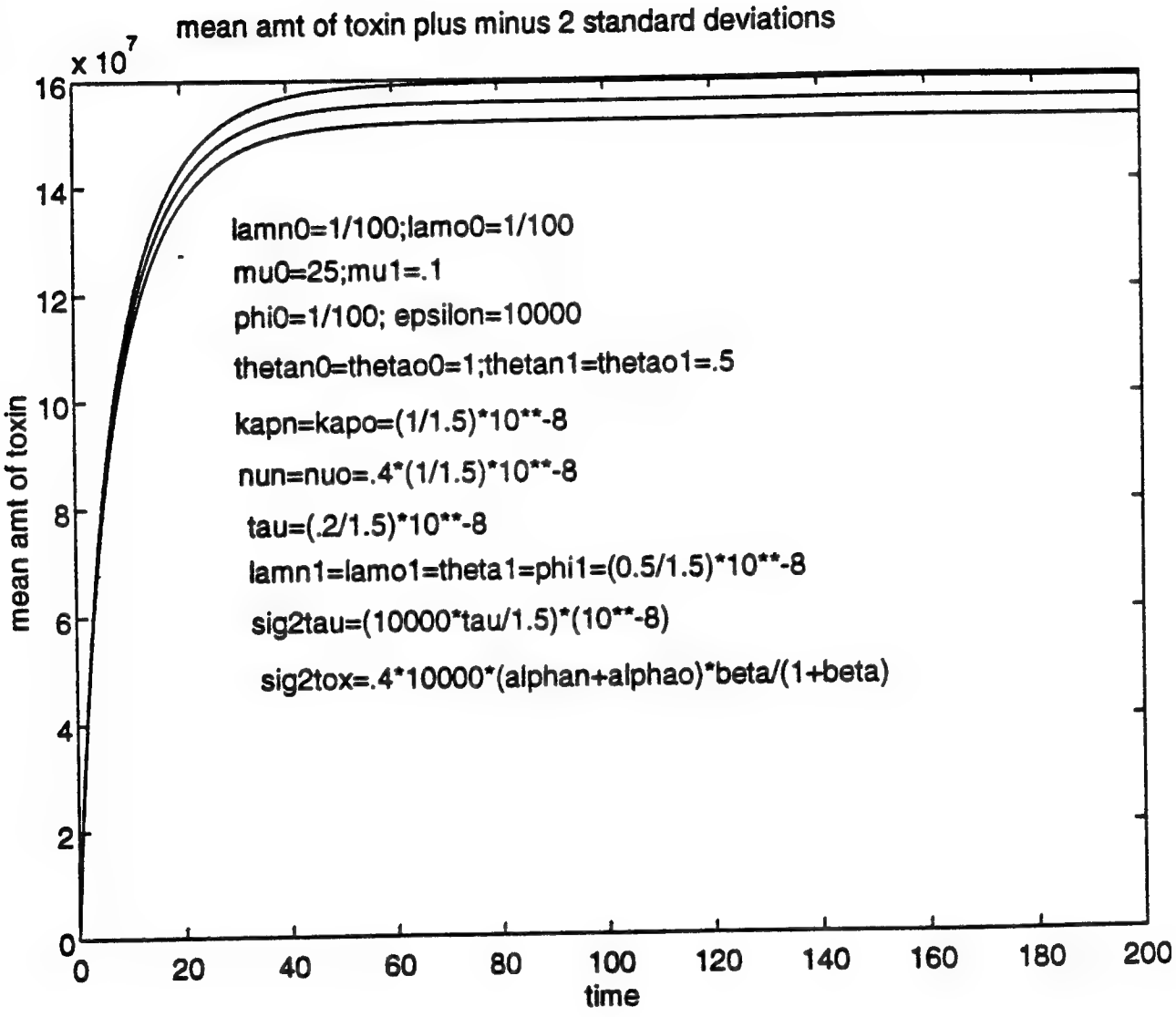
mean amt of toxin plus minus 2 standard deviations
x 10^7
mean amt of toxin
time
lamn0=1/100;lamo0=1/100
mu0=25;mu1=.1
phi0=1/100; epsilon=10000
thetan0=thetao0=1;thetan1=thetao1=.5
kapn=kapo=(1/1.5)*10**-8
nun=nuo=.4*(1/1.5)*10**-8
tau=(.2/1.5)*10**-8
lamn1=lamo1=theta1=phi1=(0.5/1.5)*10**-8
sig2tau=(10000*tau/1.5)*(10**-8)
sig2tox=.4*10000*(alphan+alphao)*beta/(1+beta)

Figure 5

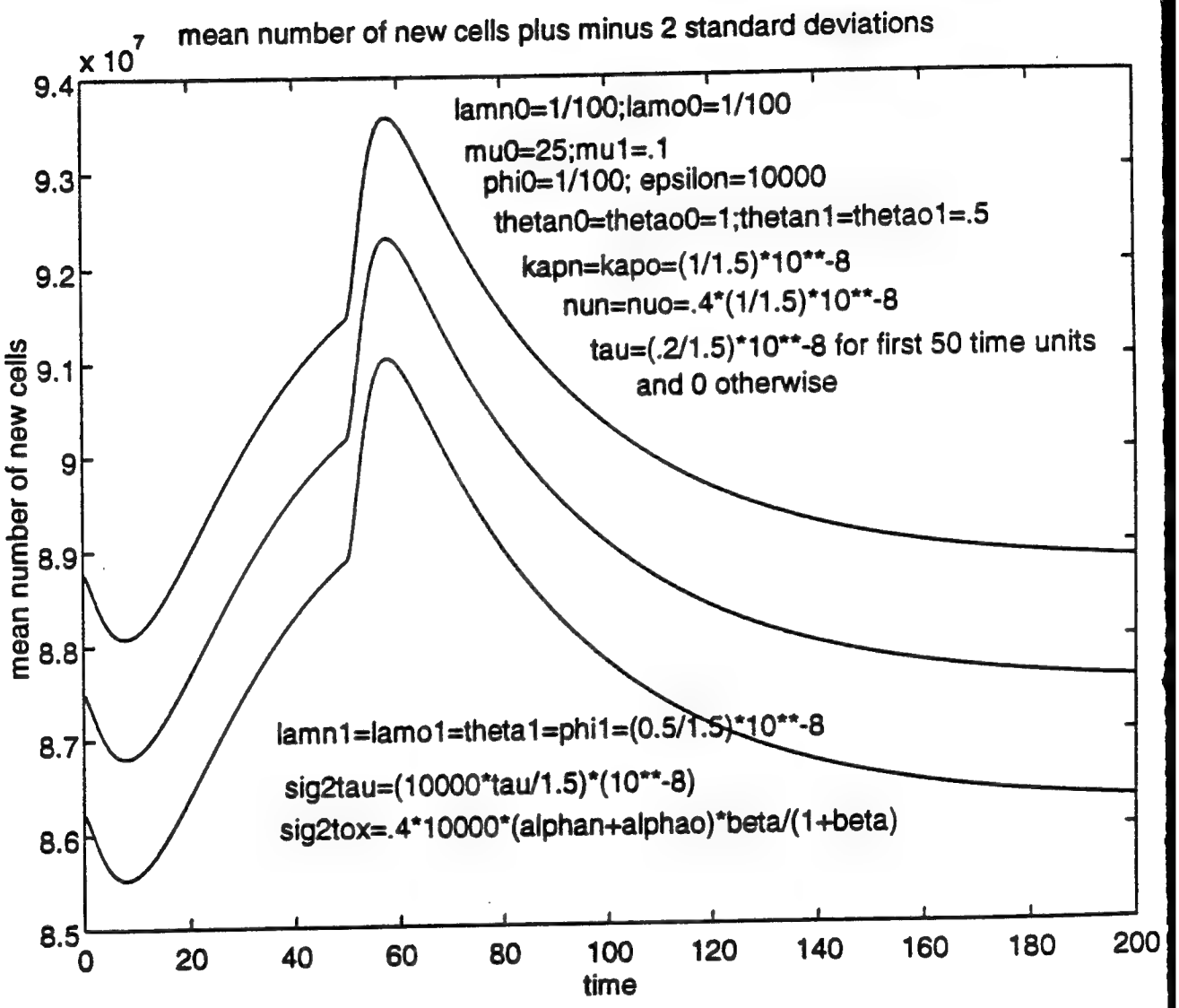
mean number of new cells plus minus 2 standard deviations
x 10^7
mean number of new cells
time
lamn0=1/100;lamo0=1/100
mu0=25;mu1=.1
phi0=1/100; epsilon=10000
thetan0=thetao0=1;thetan1=thetao1=.5
kapn=kapo=(1/1.5)*10**-8
nun=nuo=.4*(1/1.5)*10**-8
tau=(.2/1.5)*10**-8 for first 50 time units
and 0 otherwise
lamn1=lamo1=theta1=phi1=(0.5/1.5)*10**-8
sig2tau=(10000*tau/1.5)*(10**-8)
sig2tox=.4*10000*(alphan+alphao)*beta/(1+beta)
9.4
9.3
9.2
9.1
9
8.9
8.8
8.7
8.6
8.5
0
20
40
60
80
100
120
140
160
180
200

Figure 6

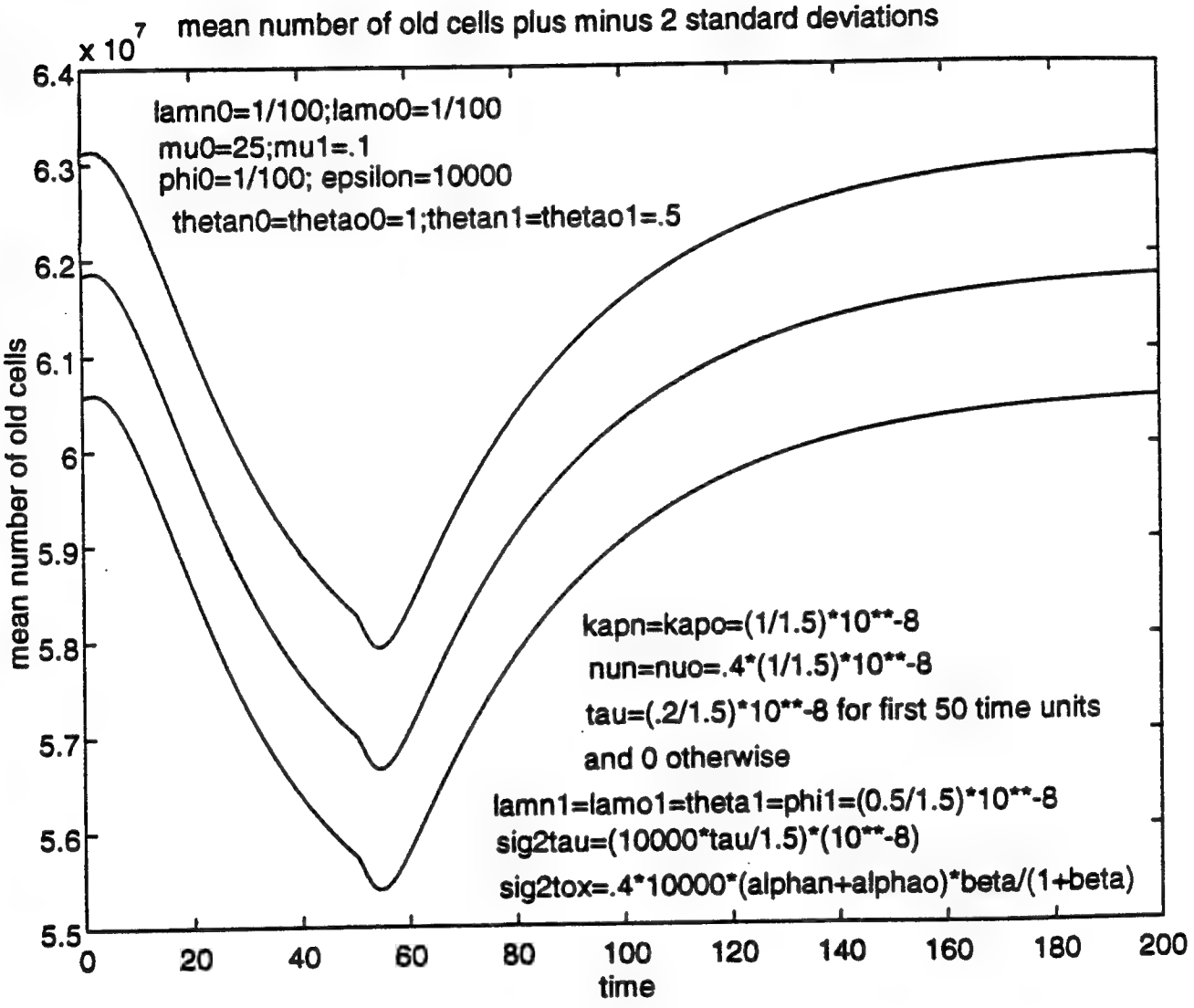
mean number of old cells plus minus 2 standard deviations
x 10^7
6.4
6.3
6.2
6.1
6
5.9
5.8
5.7
5.6
5.5
mean number of old cells
0
20
40
60
80
100
120
140
160
180
200
time
lamn0=1/100;lamo0=1/100
mu0=25;mu1=.1
phi0=1/100; epsilon=10000
thetan0=thetao0=1;thetan1=thetao1=.5
kapn=kapo=(1/1.5)*10**-8
nun=nuo=.4*(1/1.5)*10**-8
tau=(.2/1.5)*10**-8 for first 50 time units
and 0 otherwise
lamn1=lamo1=theta1=phi1=(0.5/1.5)*10**-8
sig2tau=(10000*tau/1.5)*(10**-8)
sig2tox=.4*10000*(alphan+alphao)*beta/(1+beta)

Figure 7

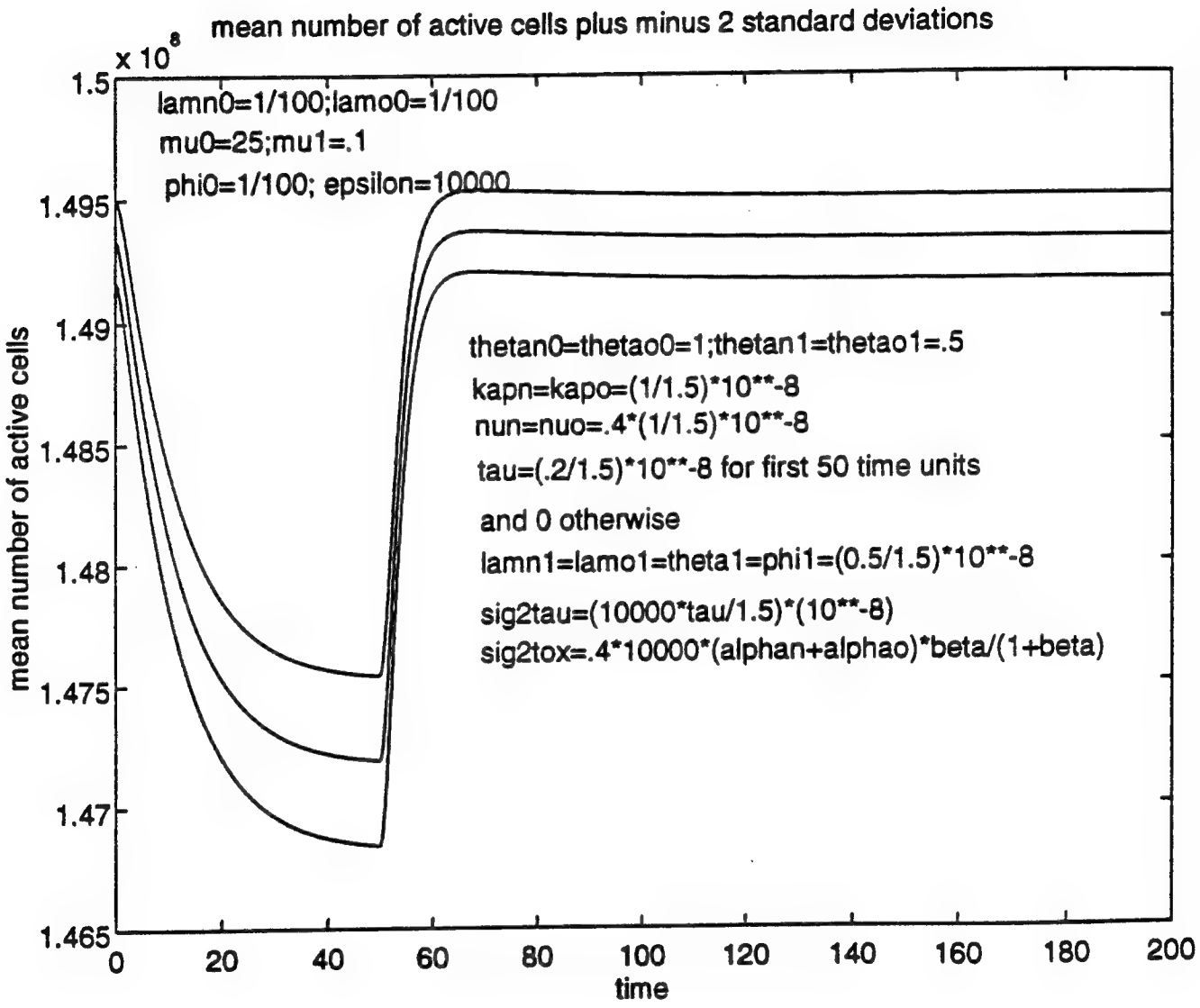
mean number of active cells plus minus 2 standard deviations
x 10^8
1.5
1.495
1.49
1.485
1.48
1.475
1.47
1.465
mean number of active cells
lamn0=1/100;lamo0=1/100
mu0=25;mu1=.1
phi0=1/100; epsilon=10000
thetan0=thetao0=1;thetan1=thetao1=.5
kapn=kapo=(1/1.5)*10**-8
nun=nuo=.4*(1/1.5)*10**-8
tau=(.2/1.5)*10**-8 for first 50 time units
and 0 otherwise
lamn1=lamo1=theta1=phi1=(0.5/1.5)*10**-8
sig2tau=(10000*tau/1.5)*(10**-8)
sig2tox=.4*10000*(alphan+alphao)*beta/(1+beta)
0
20
40
60
80
100
120
140
160
180
200
time

Figure 8

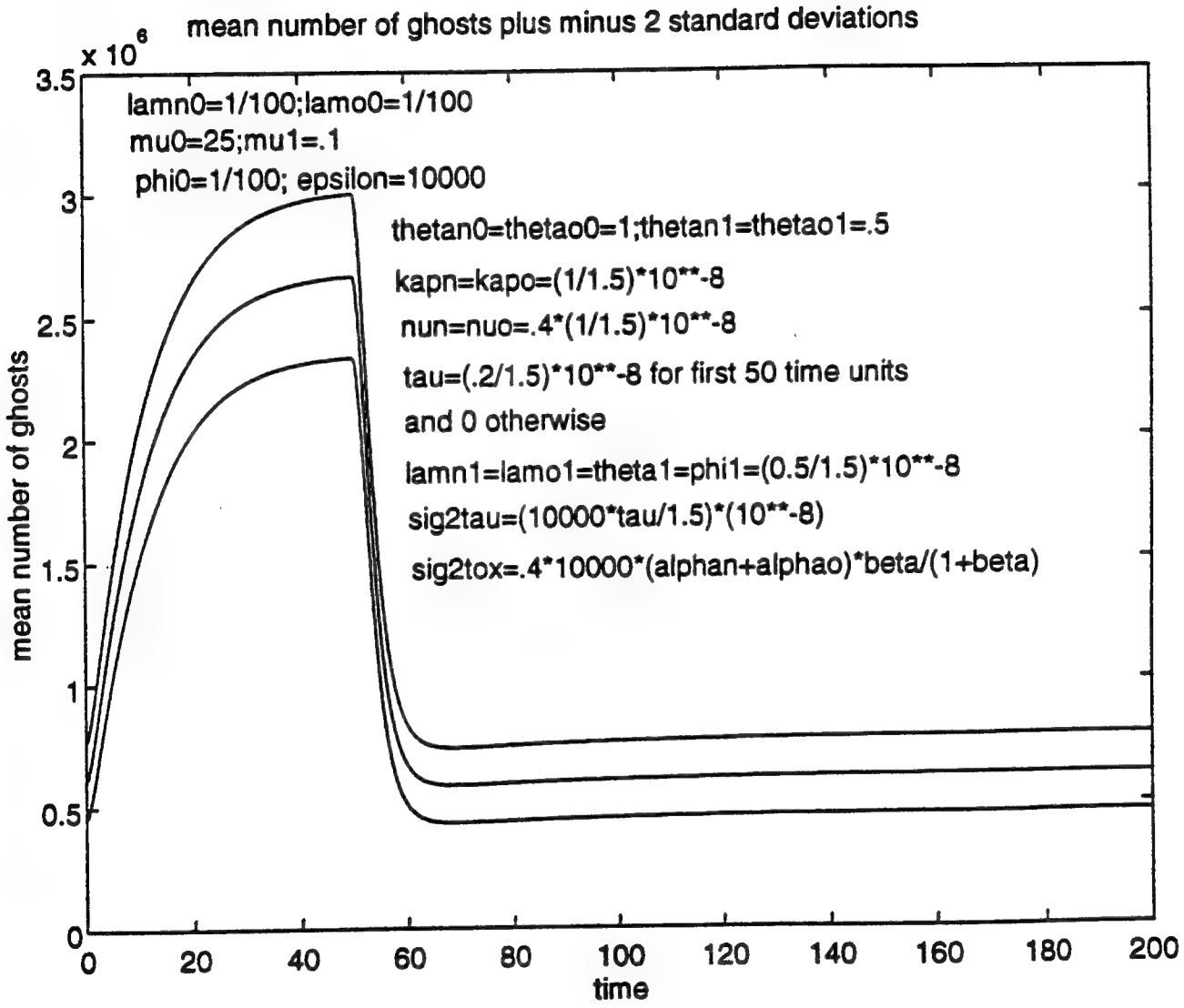
mean number of ghosts plus minus 2 standard deviations
x 10^6
lamn0=1/100;lamo0=1/100
mu0=25;mu1=.1
phi0=1/100; epsilon=10000
thetan0=thetao0=1;thetan1=thetao1=.5
kapn=kapo=(1/1.5)*10**-8
nun=nuo=.4*(1/1.5)*10**-8
tau=(.2/1.5)*10**-8 for first 50 time units
and 0 otherwise
lamn1=lamo1=theta1=phi1=(0.5/1.5)*10**-8
sig2tau=(10000*tau/1.5)*(10**-8)
sig2tox=.4*10000*(alphan+alphao)*beta/(1+beta)
mean number of ghosts
time
0
0.5
1
1.5
2
2.5
3
3.5
0
20
40
60
80
100
120
140
160
180
200

Figure 9

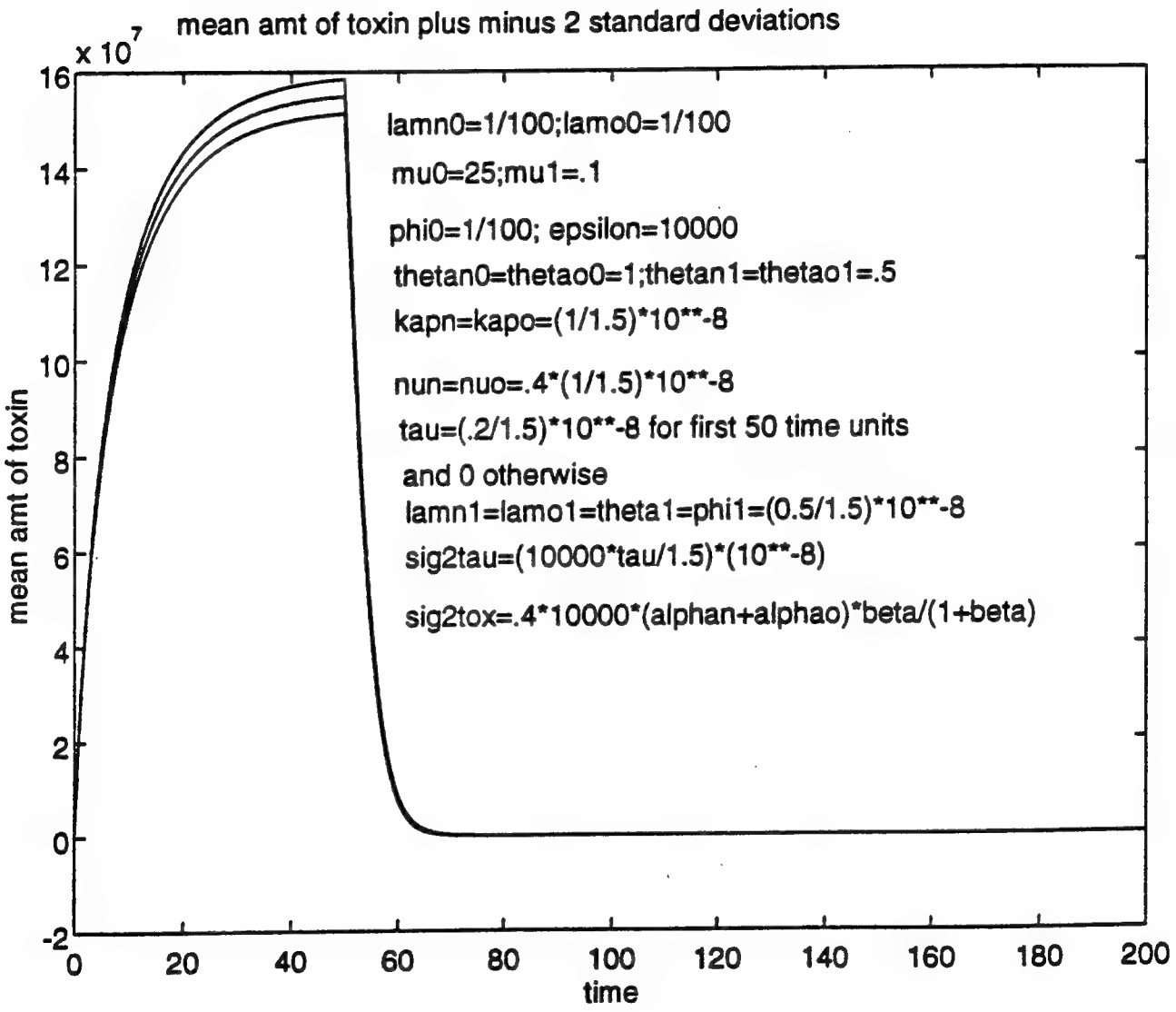
mean amt of toxin plus minus 2 standard deviations
x 10^7
16
14
12
10
8
6
4
2
0
-2
mean amt of toxin
0
20
40
60
80
100
120
140
160
180
200
time
lamn0=1/100;lamo0=1/100
mu0=25;mu1=.1
phi0=1/100; epsilon=10000
thetan0=thetao0=1;thetan1=thetao1=.5
kapn=kapo=(1/1.5)*10**-8
nun=nuo=.4*(1/1.5)*10**-8
tau=(.2/1.5)*10**-8 for first 50 time units
and 0 otherwise
lamn1=lamo1=theta1=phi1=(0.5/1.5)*10**-8
sig2tau=(10000*tau/1.5)*(10**-8)
sig2tox=.4*10000*(alphan+alphao)*beta/(1+beta)

Figure 10

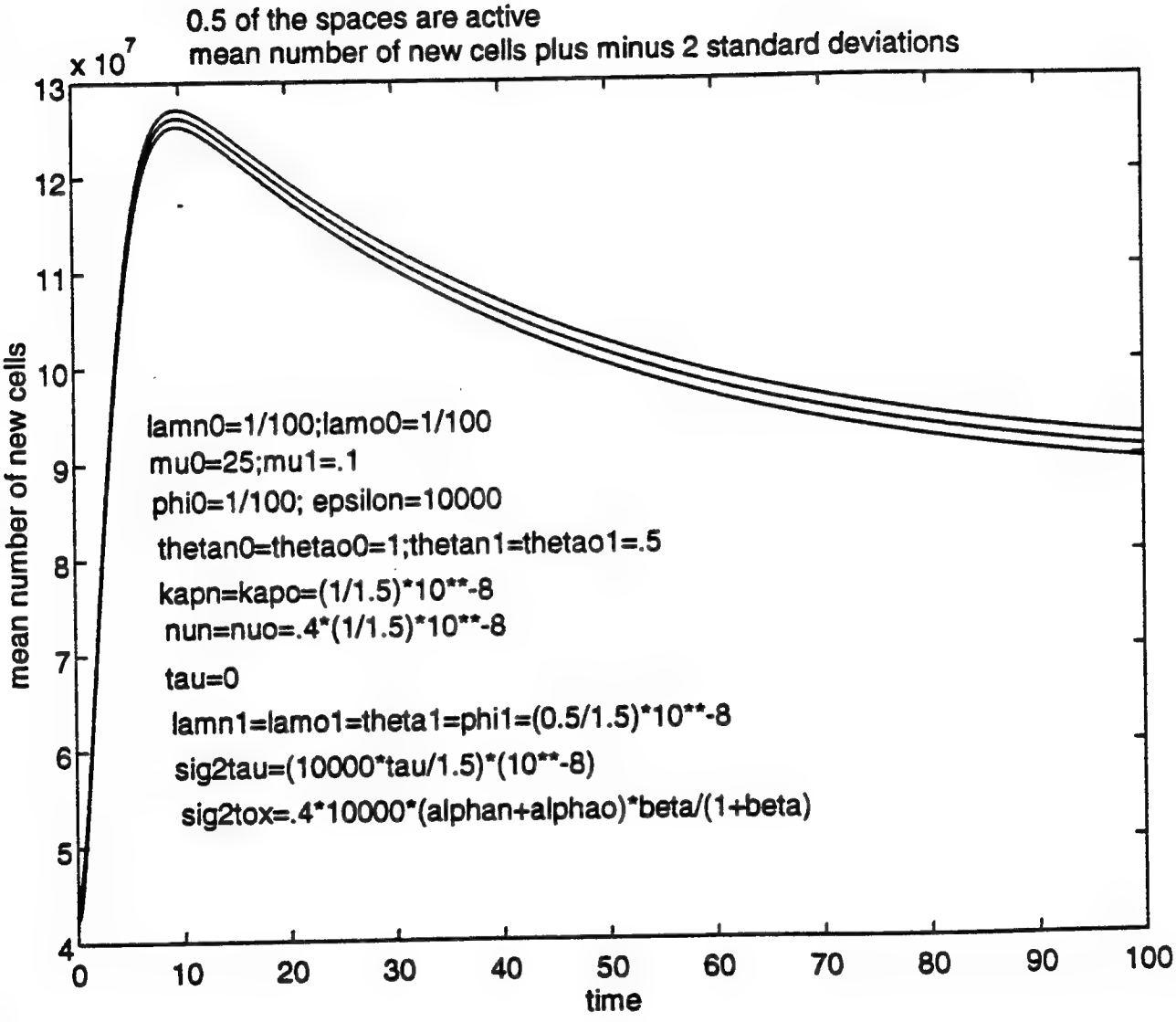
0.5 of the spaces are active
mean number of new cells plus minus 2 standard deviations
x 10^7
mean number of new cells
time
lamn0=1/100;lamo0=1/100
mu0=25;mu1=.1
phi0=1/100; epsilon=10000
thetan0=thetao0=1;thetan1=thetao1=.5
kapn=kapo=(1/1.5)*10**-8
nun=nuo=.4*(1/1.5)*10**-8
tau=0
lamn1=lamo1=theta1=phi1=(0.5/1.5)*10**-8
sig2tau=(10000*tau/1.5)*(10**-8)
sig2tox=.4*10000*(alphan+alphao)*beta/(1+beta)

Figure 11

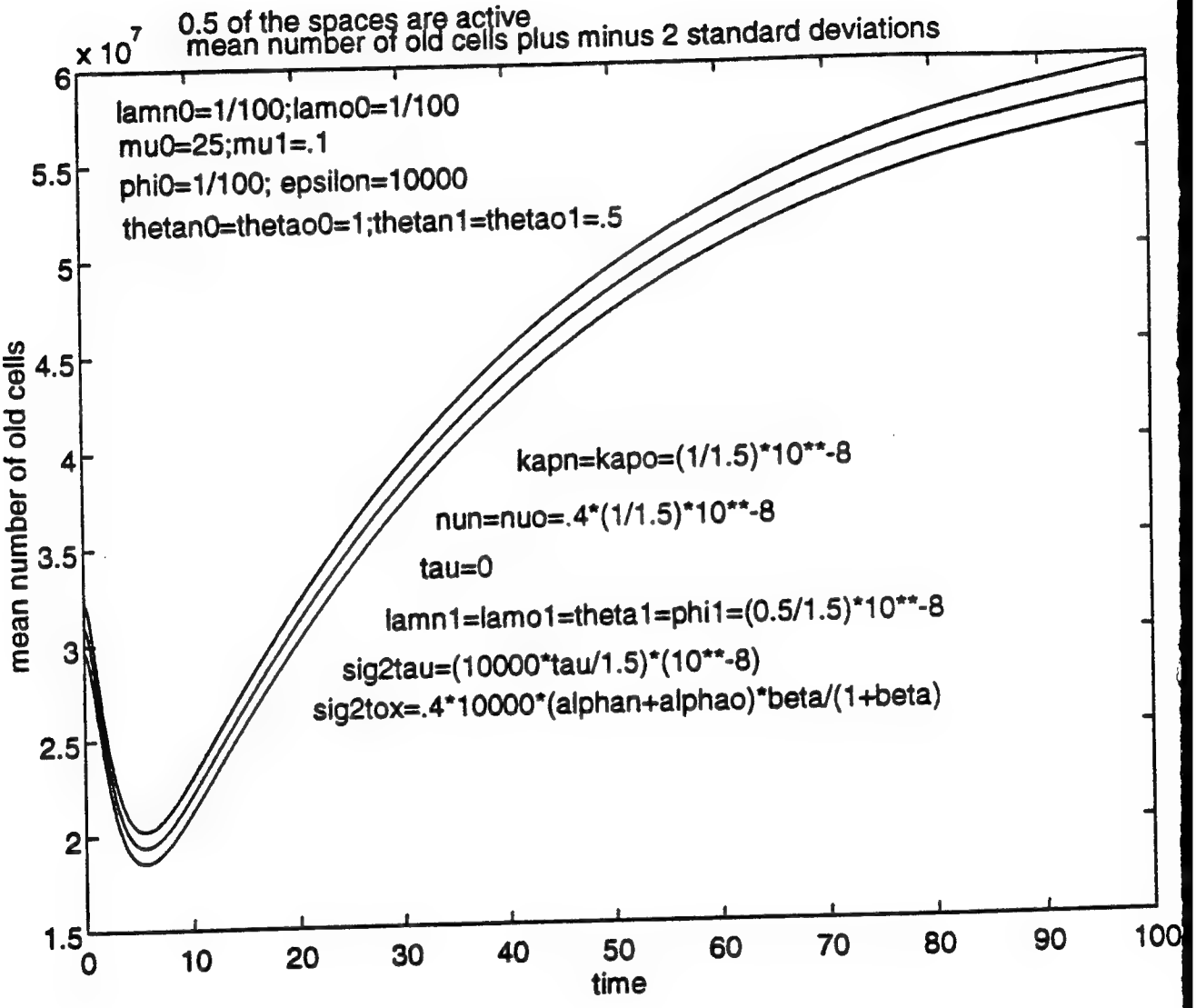
0.5 of the spaces are active
mean number of old cells plus minus 2 standard deviations
x 10^7
lamn0=1/100;lamo0=1/100
mu0=25;mu1=.1
phi0=1/100; epsilon=10000
thetan0=thetao0=1;thetan1=thetao1=.5
kapn=kapo=(1/1.5)*10**-8
nun=nuo=.4*(1/1.5)*10**-8
tau=0
lamn1=lamo1=theta1=phi1=(0.5/1.5)*10**-8
sig2tau=(10000*tau/1.5)*(10**-8)
sig2tox=.4*10000*(alphan+alphao)*beta/(1+beta)
mean number of old cells
time
6
5.5
5
4.5
4
3.5
3
2.5
2
1.5
0
10
20
30
40
50
60
70
80
90
100

Figure 12

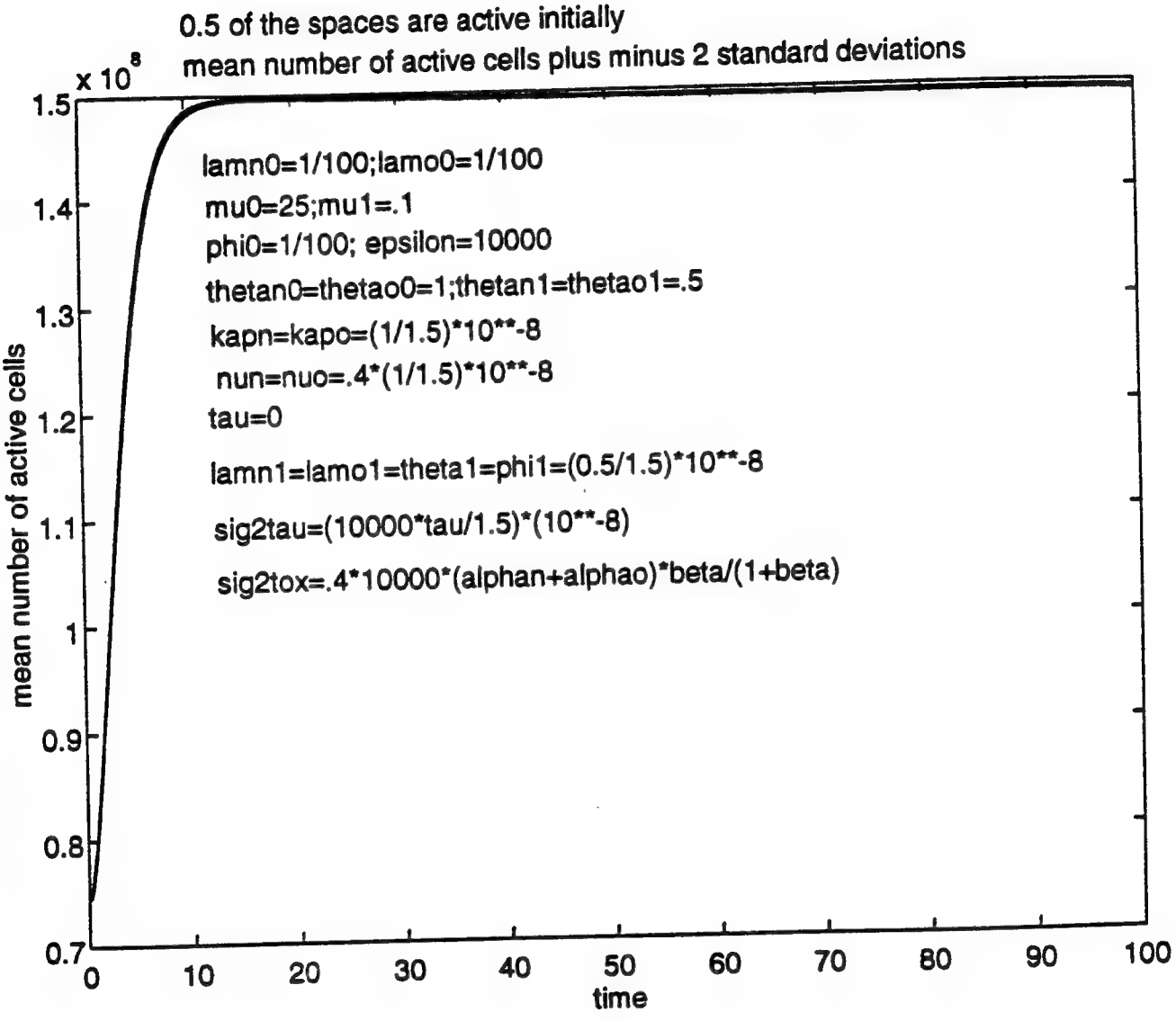
0.5 of the spaces are active initially
mean number of active cells plus minus 2 standard deviations
x 10^8
mean number of active cells
time
lamn0=1/100;lamo0=1/100
mu0=25;mu1=.1
phi0=1/100; epsilon=10000
thetan0=thetao0=1;thetan1=thetao1=.5
kapn=kapo=(1/1.5)*10**-8
nun=nuo=.4*(1/1.5)*10**-8
tau=0
lamn1=lamo1=theta1=phi1=(0.5/1.5)*10**-8
sig2tau=(10000*tau/1.5)*(10**-8)
sig2tox=.4*10000*(alphan+alphao)*beta/(1+beta)

Figure 13

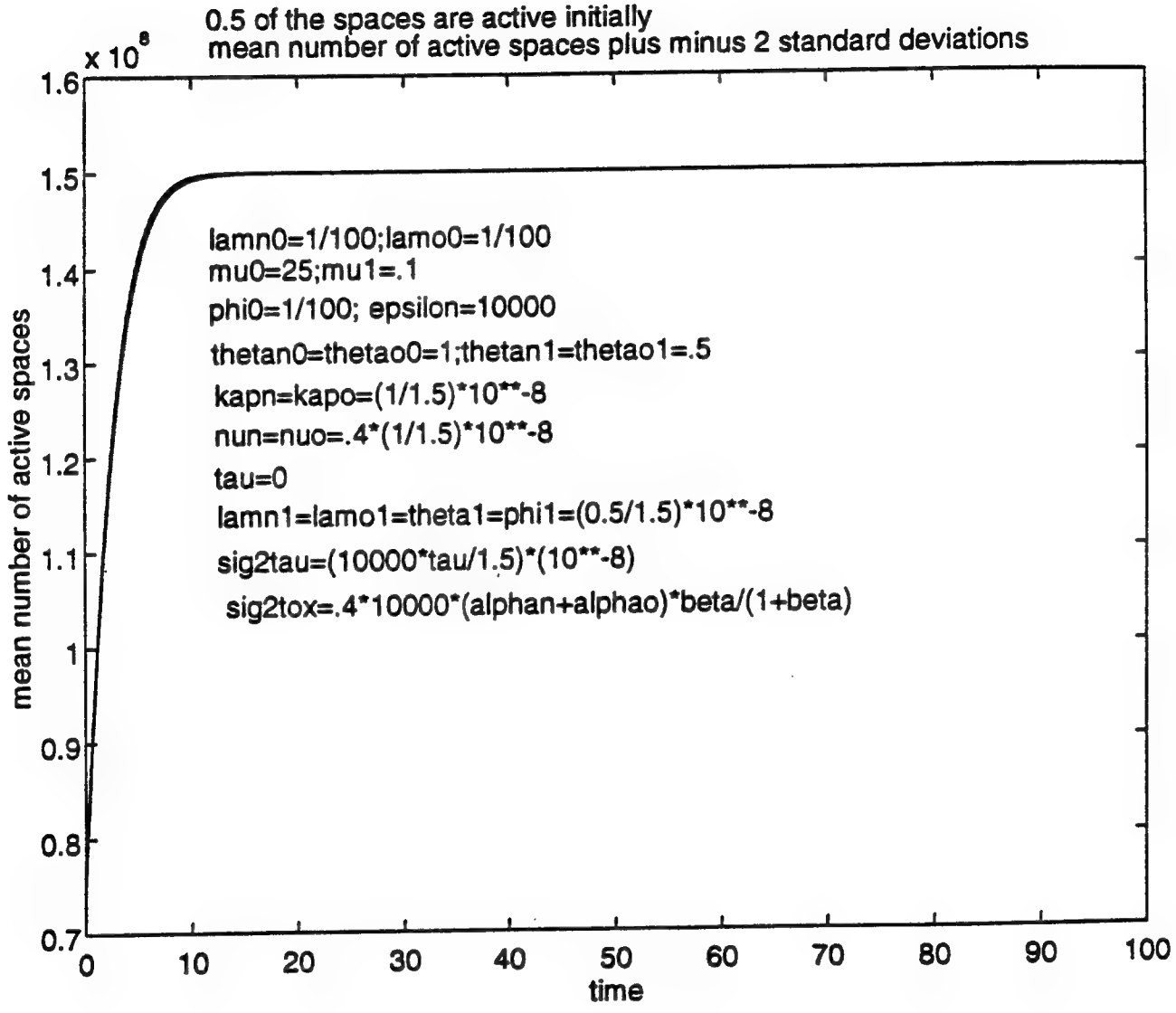
0.5 of the spaces are active initially
mean number of active spaces plus minus 2 standard deviations
x 10^8
1.6
1.5
1.4
1.3
1.2
1.1
1
0.9
0.8
0.7
mean number of active spaces
0
10
20
30
40
50
60
70
80
90
100
time
lamn0=1/100;lamo0=1/100
mu0=25;mu1=.1
phi0=1/100; epsilon=10000
thetan0=thetao0=1;thetan1=thetao1=.5
kapn=kapo=(1/1.5)*10**-8
nun=nuo=.4*(1/1.5)*10**-8
tau=0
lamn1=lamo1=theta1=phi1=(0.5/1.5)*10**-8
sig2tau=(10000*tau/1.5)*(10**-8)
sig2tox=.4*10000*(alphan+alphao)*beta/(1+beta)

Figure 14

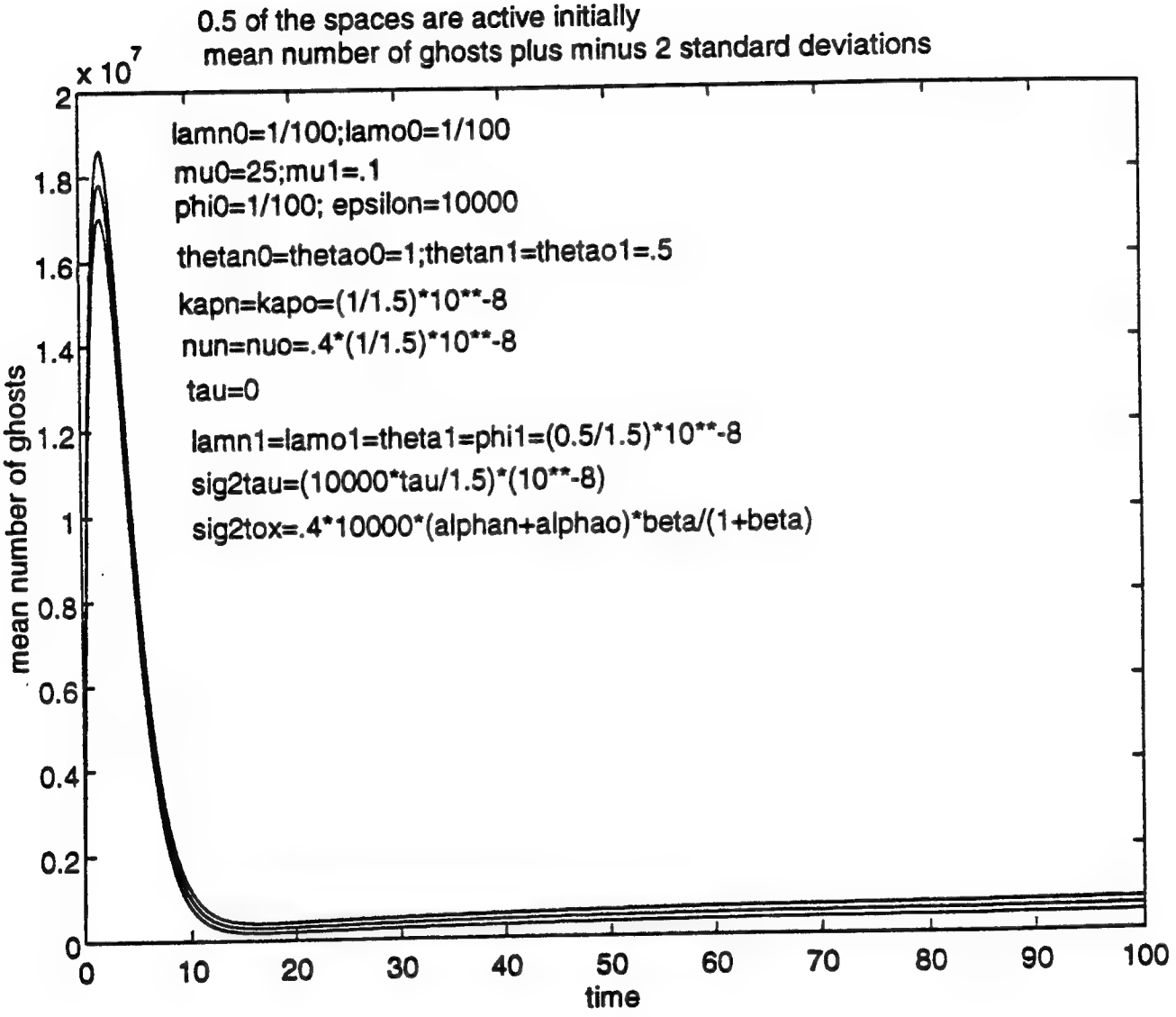
0.5 of the spaces are active initially
mean number of ghosts plus minus 2 standard deviations
x 10^7
lamn0=1/100;lamo0=1/100
mu0=25;mu1=.1
phi0=1/100; epsilon=10000
thetan0=thetao0=1;thetan1=thetao1=.5
kapn=kapo=(1/1.5)*10**-8
nun=nuo=.4*(1/1.5)*10**-8
tau=0
lamn1=lamo1=theta1=phi1=(0.5/1.5)*10**-8
sig2tau=(10000*tau/1.5)*(10**-8)
sig2tox=.4*10000*(alphan+alphao)*beta/(1+beta)
mean number of ghosts
time
0
0.2
0.4
0.6
0.8
1
1.2
1.4
1.6
1.8
2
0
10
20
30
40
50
60
70
80
90
100

Figure 15

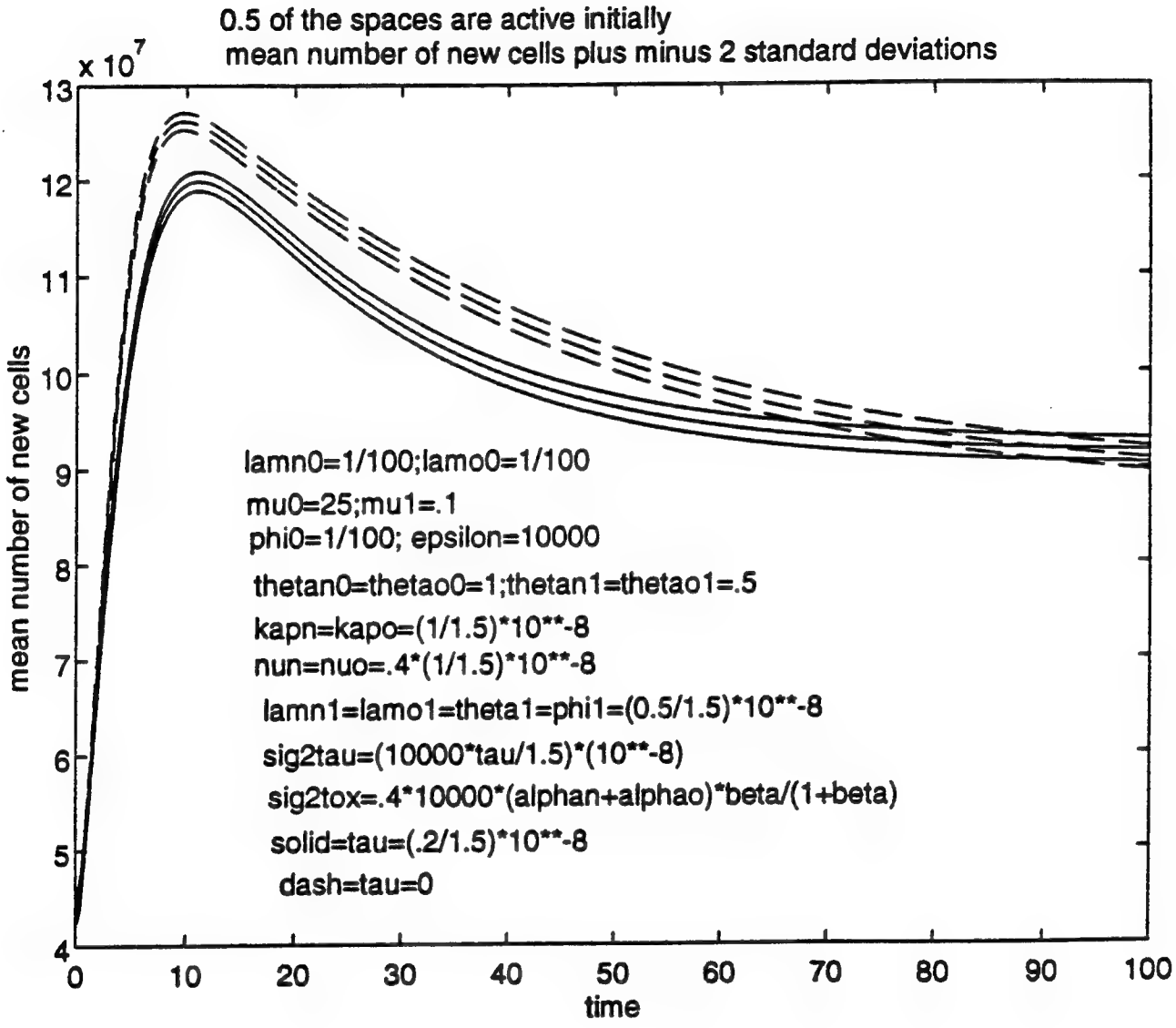
0.5 of the spaces are active initially
mean number of new cells plus minus 2 standard deviations
x 10^7
mean number of new cells
time
lamn0=1/100;lamo0=1/100
mu0=25;mu1=.1
phi0=1/100; epsilon=10000
thetan0=thetao0=1;thetan1=thetao1=.5
kapn=kapo=(1/1.5)*10**-8
nun=nuo=.4*(1/1.5)*10**-8
lamn1=lamo1=theta1=phi1=(0.5/1.5)*10**-8
sig2tau=(10000*tau/1.5)*(10**-8)
sig2tox=.4*10000*(alphan+alphao)*beta/(1+beta)
solid=tau=(.2/1.5)*10**-8
dash=tau=0

Figure 16

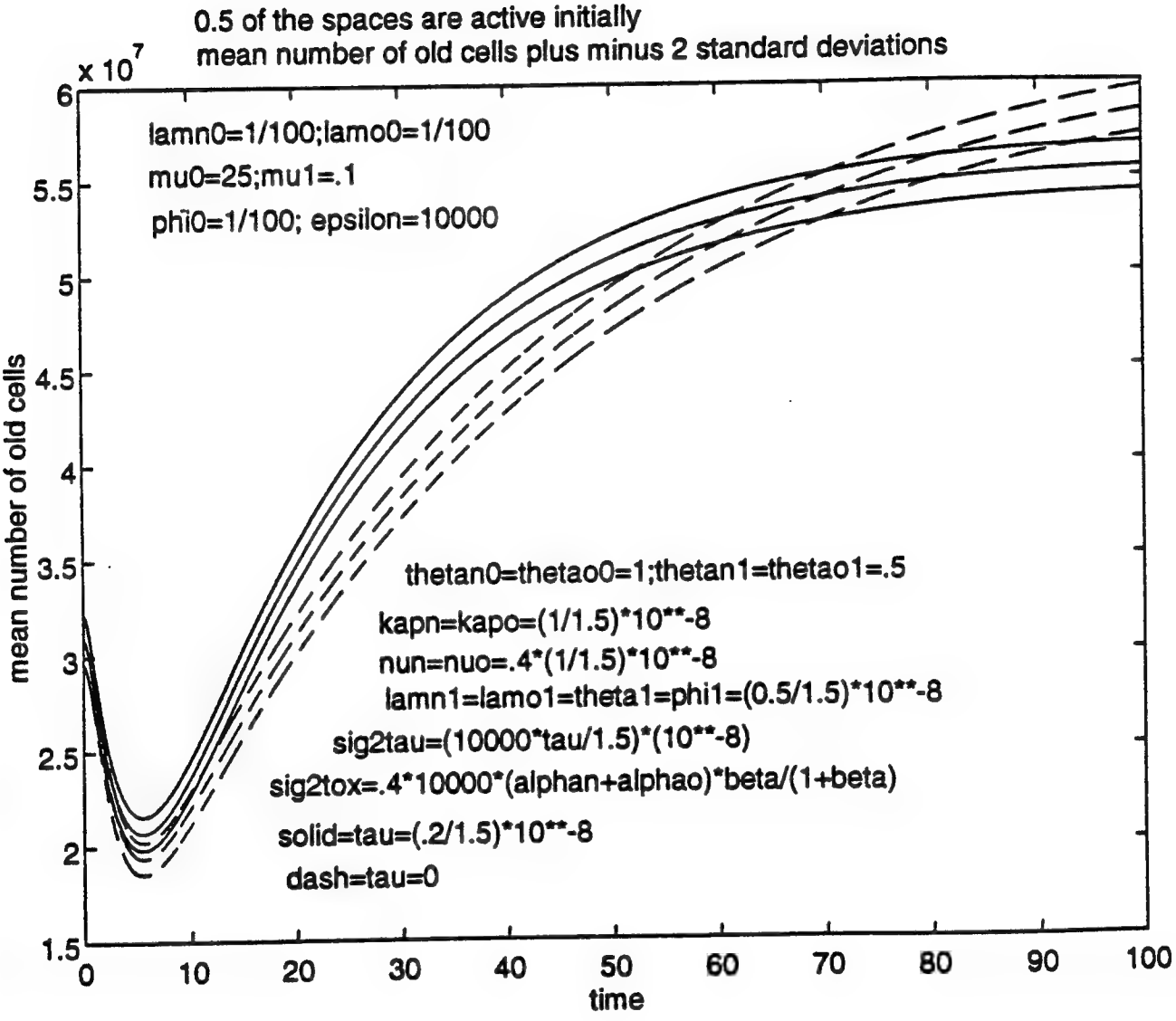
0.5 of the spaces are active initially
mean number of old cells plus minus 2 standard deviations
x 10^7
lamn0=1/100;lamo0=1/100
mu0=25;mu1=.1
phi0=1/100; epsilon=10000
thetan0=thetao0=1;thetan1=thetao1=.5
kapn=kapo=(1/1.5)*10**-8
nun=nuo=.4*(1/1.5)*10**-8
lamn1=lamo1=theta1=phi1=(0.5/1.5)*10**-8
sig2tau=(10000*tau/1.5)*(10**-8)
sig2tox=.4*10000*(alphan+alphao)*beta/(1+beta)
solid=tau=(.2/1.5)*10**-8
dash=tau=0
mean number of old cells
time
6
5.5
5
4.5
4
3.5
3
2.5
2
1.5
0
10
20
30
40
50
60
70
80
90
100

Figure 17

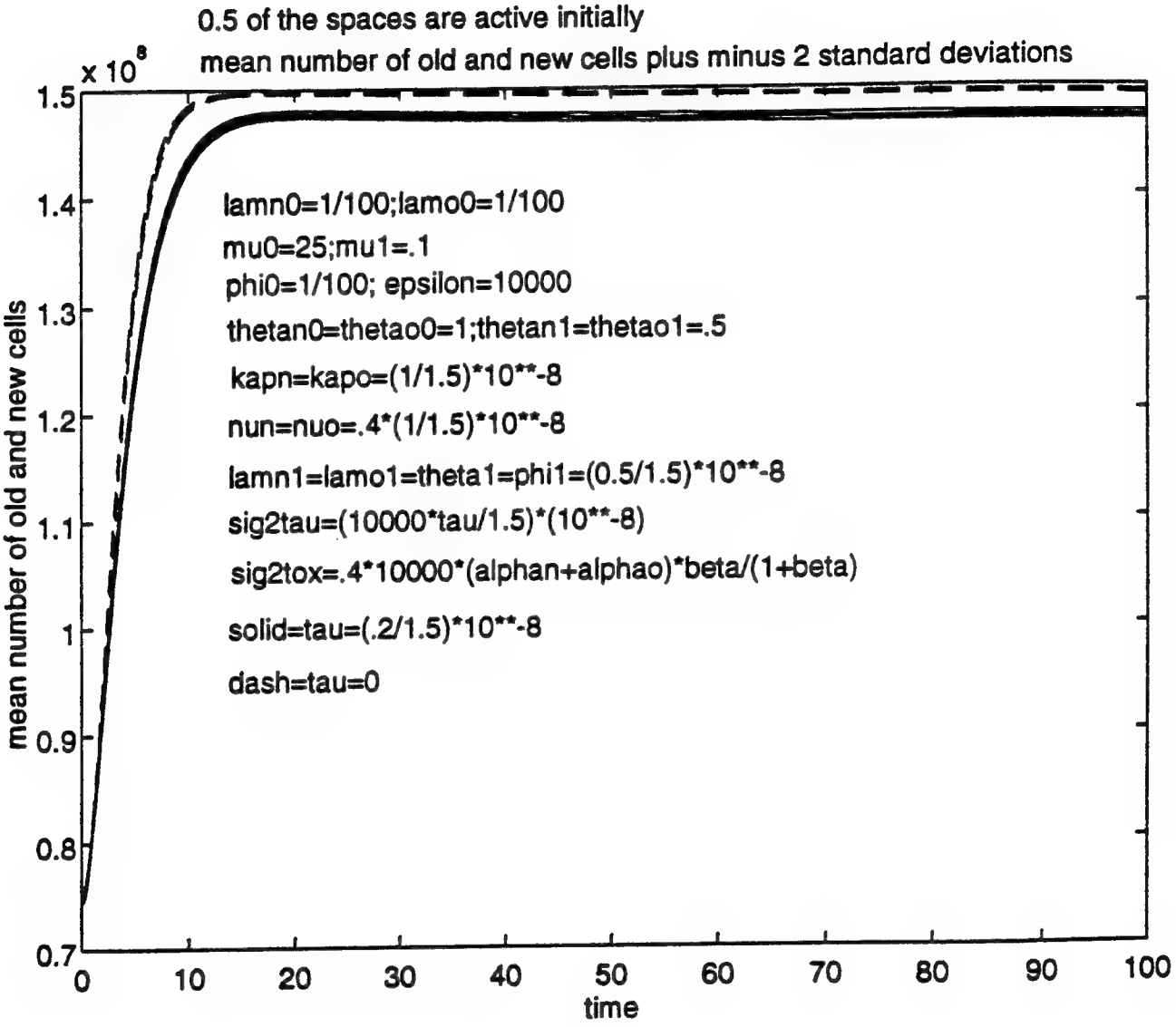
0.5 of the spaces are active initially
mean number of old and new cells plus minus 2 standard deviations
x 10^8
mean number of old and new cells
time
lamn0=1/100;lamo0=1/100
mu0=25;mu1=.1
phi0=1/100; epsilon=10000
thetan0=thetao0=1;thetan1=thetao1=.5
kapn=kapo=(1/1.5)*10**-8
nun=nuo=.4*(1/1.5)*10**-8
lamn1=lamo1=theta1=phi1=(0.5/1.5)*10**-8
sig2tau=(10000*tau/1.5)*(10**-8)
sig2tox=.4*10000*(alphan+alphao)*beta/(1+beta)
solid=tau=(.2/1.5)*10**-8
dash=tau=0

Figure 18

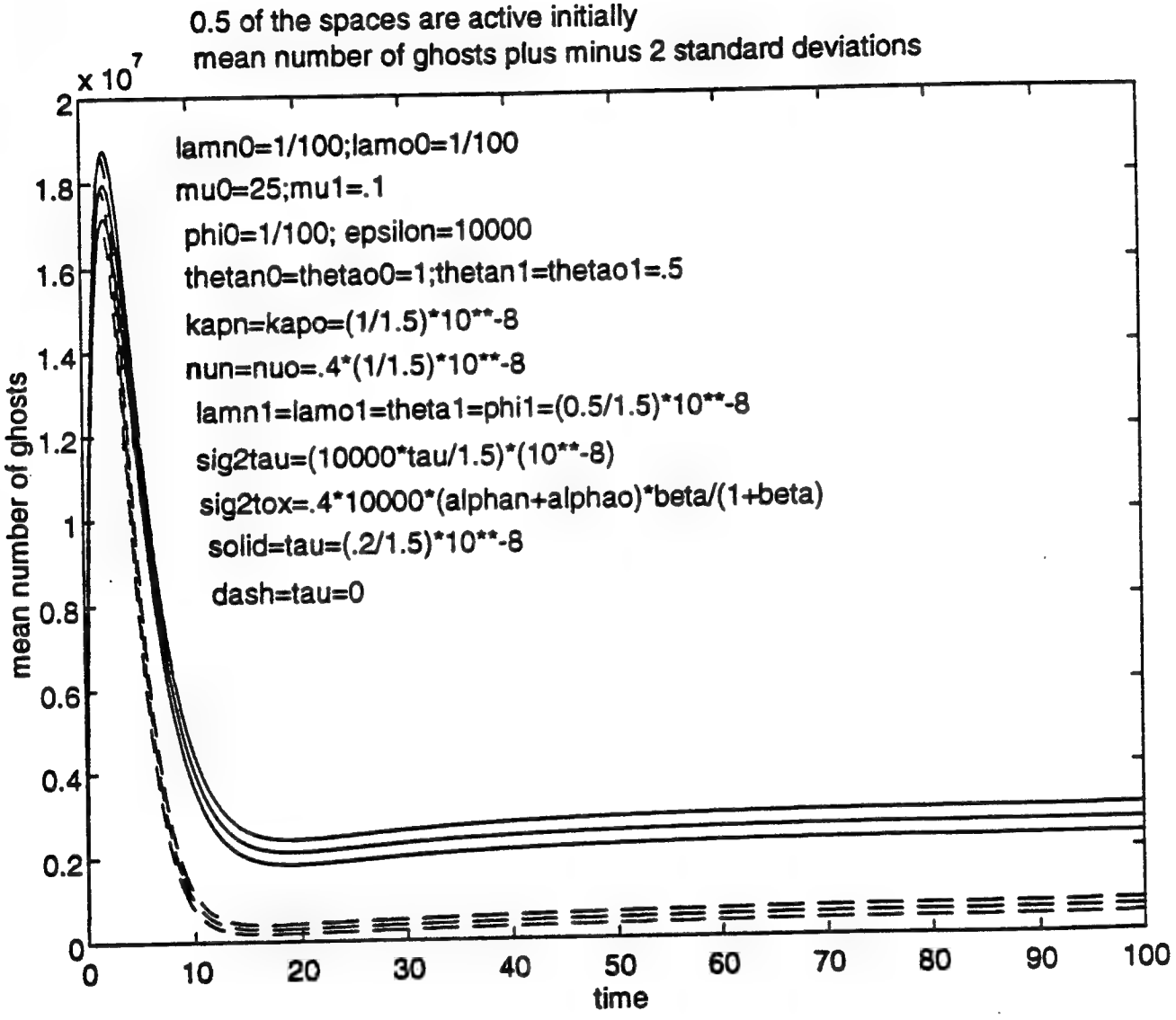
0.5 of the spaces are active initially
mean number of ghosts plus minus 2 standard deviations
x 10^7
lamn0=1/100;lamo0=1/100
mu0=25;mu1=.1
phi0=1/100; epsilon=10000
thetan0=thetao0=1;thetan1=thetao1=.5
kapn=kapo=(1/1.5)*10**-8
nun=nuo=.4*(1/1.5)*10**-8
lamn1=lamo1=theta1=phi1=(0.5/1.5)*10**-8
sig2tau=(10000*tau/1.5)*(10**-8)
sig2tox=.4*10000*(alphan+alphao)*beta/(1+beta)
solid=tau=(.2/1.5)*10**-8
dash=tau=0
mean number of ghosts
time
0
0.2
0.4
0.6
0.8
1
1.2
1.4
1.6
1.8
2
0
10
20
30
40
50
60
70
80
90
100

Figure 19

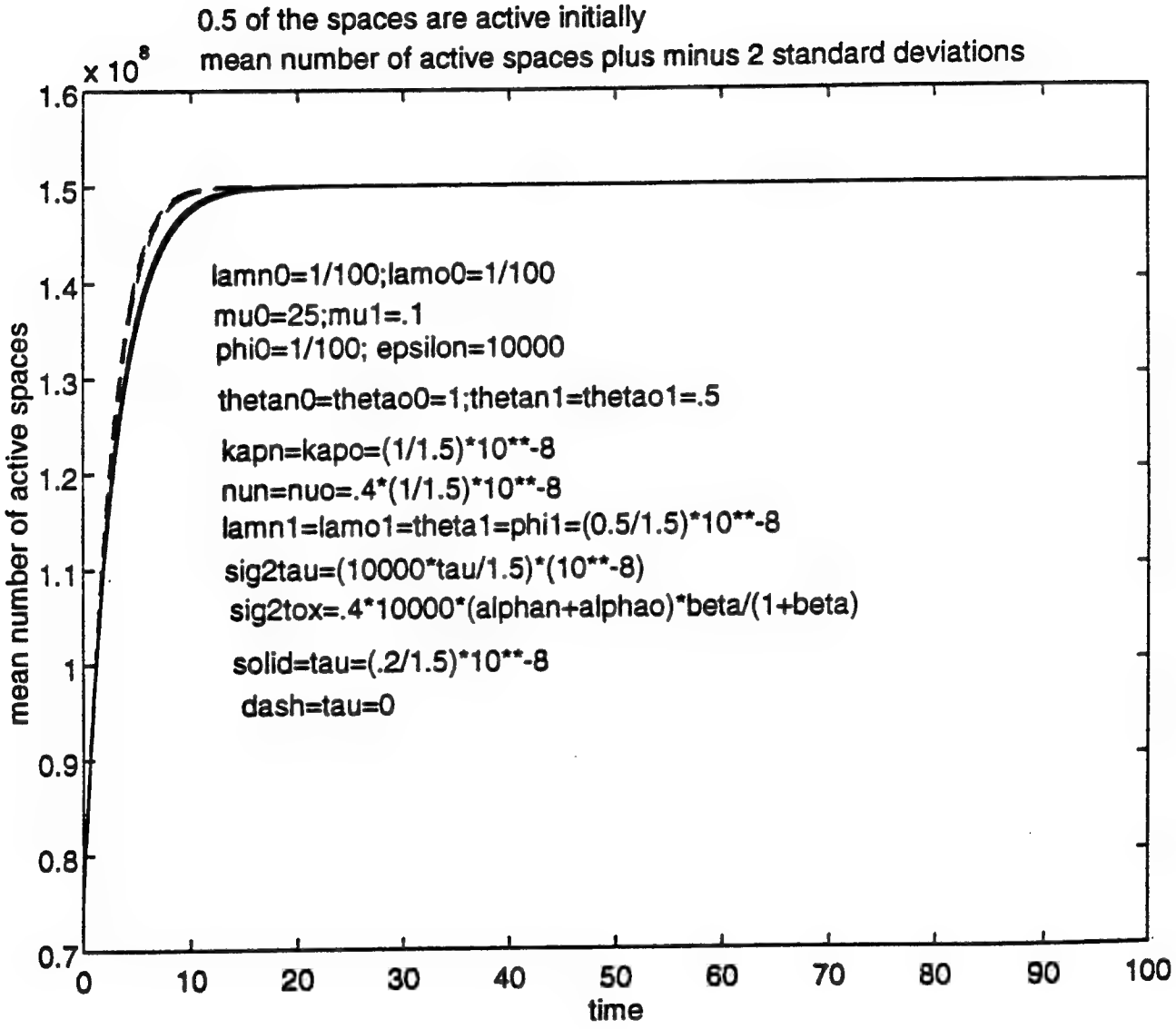
0.5 of the spaces are active initially
mean number of active spaces plus minus 2 standard deviations
x 10^8
mean number of active spaces
time
lamn0=1/100;lamo0=1/100
mu0=25;mu1=.1
phi0=1/100; epsilon=10000
thetan0=thetao0=1;thetan1=thetao1=.5
kapn=kapo=(1/1.5)*10**-8
nun=nuo=.4*(1/1.5)*10**-8
lamn1=lamo1=theta1=phi1=(0.5/1.5)*10**-8
sig2tau=(10000*tau/1.5)*(10**-8)
sig2tox=.4*10000*(alphan+alphao)*beta/(1+beta)
solid=tau=(.2/1.5)*10**-8
dash=tau=0

Figure 20

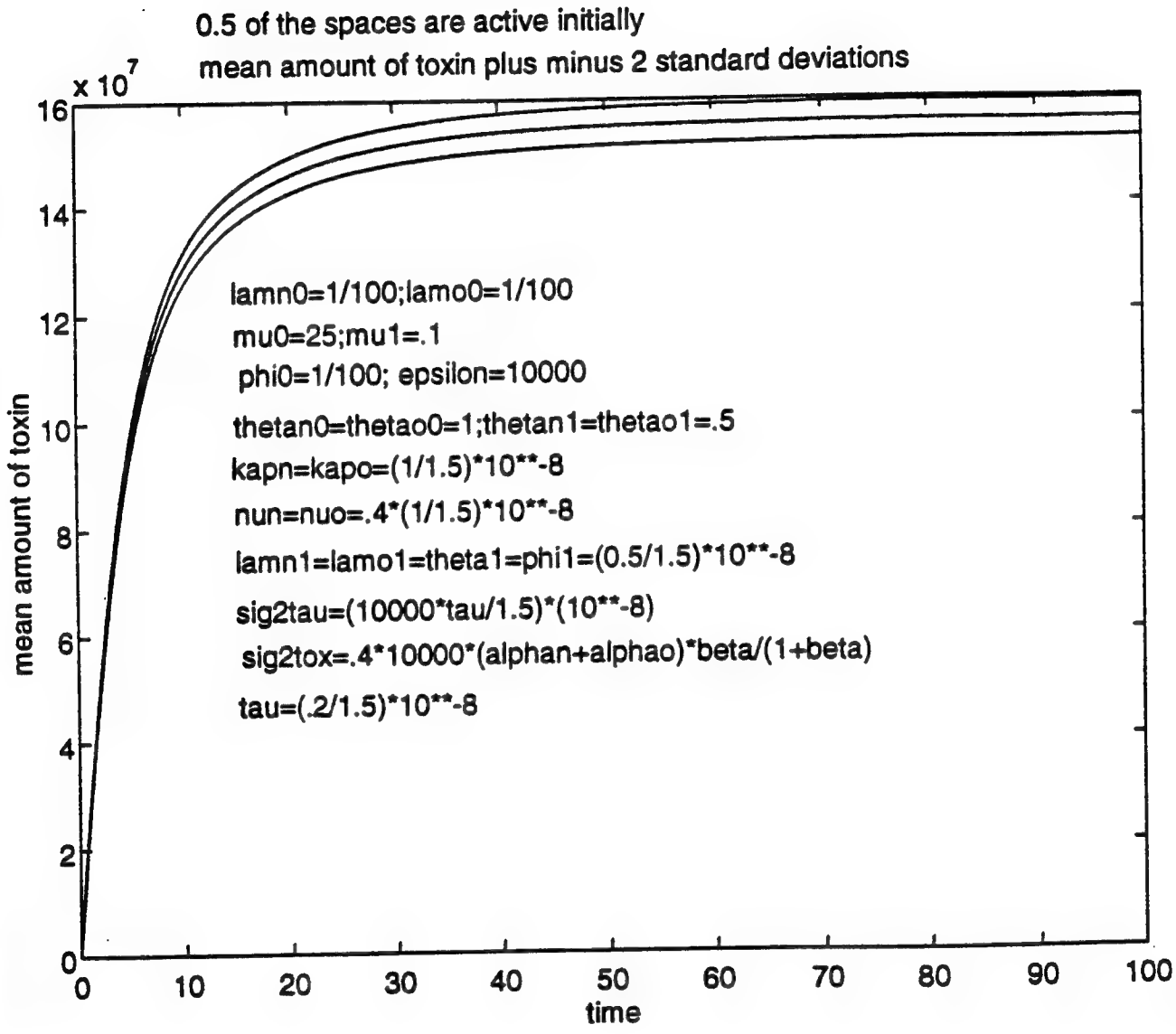
0.5 of the spaces are active initially
mean amount of toxin plus minus 2 standard deviations
x 10^7
mean amount of toxin
time
lamn0=1/100;lamo0=1/100
mu0=25;mu1=.1
phi0=1/100; epsilon=10000
thetan0=thetao0=1;thetan1=thetao1=.5
kapn=kapo=(1/1.5)*10**-8
nun=nuo=.4*(1/1.5)*10**-8
lamn1=lamo1=theta1=phi1=(0.5/1.5)*10**-8
sig2tau=(10000*tau/1.5)*(10**-8)
sig2tox=.4*10000*(alphan+alphao)*beta/(1+beta)
tau=(.2/1.5)*10**-8

Figure 21

Appendix 1

This appendix provides the detailed asymptotic development of both the deterministic approximation (5.5) – (5.9) but also for the stochastic components introduced in (6.7). Start by introducing the normalization (6.7) into (6.1) – (6.5) and divide by C_0. The following results are obtained:

$$
\begin{aligned}
d\alpha_n(t)+\frac{1}{\sqrt{C_0}}dX_n(t) &= -\left[\lambda_n(\beta(t))+\lambda_n'(\beta(t))\frac{Y(t)}{\sqrt{C_0}}\right]\left[\alpha_n(t)+\frac{1}{\sqrt{C_0}}X_n(t)\right]dt \\
&-\left[\theta_n(\beta(t))+\theta_n'(\beta(t))\frac{Y(t)}{\sqrt{C_0}}\right]\left[\gamma(t)+\frac{1}{\sqrt{C_0}}X_g(t)\right]\left[\frac{\alpha_n(t)+\frac{1}{\sqrt{C_0}}X_n(t)}{\eta(t)+\frac{1}{\sqrt{C_0}}X_c(t)}\right]dt \\
&-\left[\phi(\beta(t))+\phi'(\beta(t))\frac{Y(t)}{\sqrt{C_0}}\right]\left[\alpha_n(t)+\frac{1}{\sqrt{C_0}}X_n(t)\right]dt \\
&+\left[\mu(\beta(t))+\mu'(\beta(t))\frac{Y(t)}{\sqrt{C_0}}\right]\left\{\left[\eta(t)-\alpha_n(t)-\alpha_o(t)-\gamma(t)\right]\right. \\
&\left.+\frac{1}{\sqrt{C_0}}\left[X_c(t)-X_n(t)-X_o(t)-X_g(t)\right]\right\}dt \\
&-\frac{1}{\sqrt{C_0}}\sqrt{\varepsilon\lambda_n(\beta(t))\alpha_n(t)}\,dW_{\lambda_n}(t)-\frac{1}{\sqrt{C_0}}\sqrt{\varepsilon\phi(\beta(t))\alpha_n(t)}\,dW_{\phi}(t) \\
&-\frac{1}{\sqrt{C_0}}\sqrt{\varepsilon\theta_n(\beta(t))\gamma(t)\frac{\alpha_n(t)}{\eta(t)}}\,dW_{\theta_n}(t) \\
&+\frac{1}{\sqrt{C_0}}\sqrt{\varepsilon 4\mu(\beta(t))(\eta(t)-\alpha_n(t)-\alpha_o(t)-\gamma(t))\frac{1}{2}}\,dW_{\mu}(t)+o\left(\frac{1}{\sqrt{C_0}}\right)
\end{aligned}
\tag{A.1}
$$

$$d\alpha_o(t)+\frac{1}{\sqrt{C_0}}dX_o(t)=-\left[\lambda_o(\beta(t))+\lambda_o'(\beta(t))\frac{Y(t)}{\sqrt{C_0}}\right]\left[\alpha_o(t)+\frac{1}{\sqrt{C_0}}X_o(t)\right]dt$$

$$-\left[\theta_o(\beta(t))+\theta_o'(\beta(t))\frac{Y(t)}{\sqrt{C_0}}\right]\left[\gamma(t)+\frac{1}{\sqrt{C_0}}X_g(t)\right]\left[\frac{\alpha_o(t)+\frac{1}{\sqrt{C_0}}X_o(t)}{\eta(t)+\frac{1}{\sqrt{C_0}}X_c(t)}\right]dt$$

$$+\left[\phi(\beta(t))+\phi'(\beta(t))\frac{Y(t)}{\sqrt{C_0}}\right]\left[\alpha_n(t)+\frac{1}{\sqrt{C_0}}X_n(t)\right]dt \qquad \text{(A.2)}$$

$$-\frac{1}{\sqrt{C_0}}\sqrt{\varepsilon\lambda_o(\beta(t))\alpha_o(t)}\,dW_{\lambda_o}(t)+\frac{1}{\sqrt{C_0}}\sqrt{\varepsilon\phi(\beta(t))\alpha_n(t)}\,dW_{\phi}(t)$$

$$-\frac{1}{\sqrt{C_0}}\sqrt{\varepsilon\theta_o(\beta(t))\gamma(t)\frac{\alpha_o(t)}{\eta(t)}}\,dW_{\theta_o}(t)+o\left(\frac{1}{\sqrt{C_0}}\right)$$

$$d\gamma(t)+\frac{1}{\sqrt{C_0}}dX_g(t)=$$

$$-\left[\theta_n(\beta(t))+\theta_n'(\beta(t))\frac{Y(t)}{\sqrt{C_0}}\right]\left[\gamma(t)+\frac{1}{\sqrt{C_0}}X_g(t)\right]\left[\frac{\alpha_n(t)+\frac{1}{\sqrt{C_0}}X_n(t)}{\eta(t)+\frac{1}{\sqrt{C_0}}X_c(t)}\right]dt$$

$$-\left[\theta_o(\beta(t))+\theta_o'(\beta(t))\frac{Y(t)}{\sqrt{C_0}}\right]\left[\gamma(t)+\frac{1}{\sqrt{C_0}}X_g(t)\right]\left[\frac{\alpha_o(t)+\frac{1}{\sqrt{C_0}}X_o(t)}{\eta(t)+\frac{1}{\sqrt{C_0}}X_c(t)}\right]dt$$

$$+\left[\xi_n(\beta(t))+\xi_n'(\beta(t))\frac{Y(t)}{\sqrt{C_0}}\right]\left[\alpha_n(t)+\frac{1}{\sqrt{C_0}}X_n(t)\right]\left[1-\eta(t)-\frac{1}{\sqrt{C_0}}X_c(t)\right]dt$$

$$+\left[\xi_o(\beta(t))+\xi_o'(\beta(t))\frac{Y(t)}{\sqrt{C_0}}\right]\left[\alpha_o(t)+\frac{1}{\sqrt{C_0}}X_o(t)\right]\left[1-\eta(t)-\frac{1}{\sqrt{C_0}}X_c(t)\right]dt$$

$$+\left[\lambda_o(\beta(t))+\lambda_o'(\beta(t))\frac{Y(t)}{\sqrt{C_0}}\right]\left[\alpha_o(t)+\frac{1}{\sqrt{C_0}}X_o(t)\right]dt$$

$$+\left[\lambda_n(\beta(t))+\lambda_n'(\beta(t))\frac{Y(t)}{\sqrt{C_0}}\right]\left[\alpha_n(t)+\frac{1}{\sqrt{C_0}}X_n(t)\right]dt$$

$$-\frac{1}{\sqrt{C_0}}\sqrt{\varepsilon\theta_n(\beta(t))\gamma(t)\alpha_n(t)/\eta(t)}\,dW_{\theta_n}(t)$$

$$-\frac{1}{\sqrt{C_0}}\sqrt{\varepsilon\theta_o(\beta(t))\gamma(t)\alpha_o(t)/\eta(t)}\,dW_{\theta_o}(t)$$

$$+\frac{1}{\sqrt{C_0}}\sqrt{\varepsilon\lambda_o(\beta(t))\alpha_o(t)}\,dW_{\lambda_o}(t)+\frac{1}{\sqrt{C_0}}\sqrt{\varepsilon\lambda_n(\beta(t))\alpha_n(t)}\,dW_{\lambda_n}(t) \qquad \text{(A.3)}$$

$$+\frac{1}{\sqrt{C_0}}\sqrt{\varepsilon\xi_n(\beta(t))\alpha_n(t)[1-\eta(t)]}\,dW_{\xi_n}(t)$$

$$+\frac{1}{\sqrt{C_0}}\sqrt{\varepsilon\xi_o(\beta(t))\alpha_o(t)[1-\eta(t)]}\,dW_{\xi_o}(t)+o\left(\frac{1}{\sqrt{C_0}}\right)$$

$$d\eta(t)+\frac{1}{\sqrt{C_0}}dX_c(t)=$$

$$\left[\xi_o(\beta(t))+\xi_o'(\beta(t))\frac{1}{\sqrt{C_0}}Y(t)\right]\left[\alpha_o(t)+\frac{1}{\sqrt{C_0}}X_o(t)\right]\left[1-\eta(t)-\frac{1}{\sqrt{C_0}}X_c(t)\right]dt$$

$$+\left[\xi_n(\beta(t))+\xi_n'(\beta(t))\frac{1}{\sqrt{C_0}}Y(t)\right]\left[\alpha_n(t)+\frac{1}{\sqrt{C_0}}X_n(t)\right]\left[1-\eta(t)-\frac{1}{\sqrt{C_0}}X_c(t)\right]dt \qquad \text{(A.4)}$$

$$+\frac{1}{\sqrt{C_0}}\sqrt{\varepsilon\xi_o(\beta(t))\alpha_o(t)[1-\eta(t)]}\,dW_{\xi_o}(t)$$

$$+\frac{1}{\sqrt{C_0}}\sqrt{\varepsilon\xi_n(\beta(t))\alpha_n(t)[1-\eta(t)]}\,dW_{\xi_n}(t)+o\left(\frac{1}{\sqrt{C_0}}\right)$$

$$\frac{d\beta(t)}{dt}+\frac{1}{\sqrt{C_0}}\frac{dY(t)}{dt}=\delta(\alpha_n(t),\alpha_o(t),\beta(t),\tau(t))$$

$$+\delta_\beta'(\alpha_n(t),\alpha_o(t),\beta(t),\tau(t))\frac{Y(t)}{\sqrt{C_0}}$$

$$+\delta_{\alpha_n}'(\alpha_n(t),\alpha_o(t),\beta(t),\tau(t))\frac{X_n(t)}{\sqrt{C_0}}$$

$$+\delta_{\alpha_o}'(\alpha_n(t),\alpha_o(t),\beta(t),\tau(t))\frac{X_o(t)}{\sqrt{C_0}} \qquad \text{(A.5)}$$

$$+\frac{1}{\sqrt{C_0}}\sigma_T(\beta(t),\alpha_n(t),\alpha_o(t),\tau(t))dW_{\sigma_T}(t)$$

$$+\frac{1}{\sqrt{C_0}}\sigma_\tau\,dW_\tau(t)+o\left(\frac{1}{\sqrt{C_0}}\right)$$

The terms of order 1 in (A.1) – (A.5) yield the deterministic equations (5.5) – (5.9).

The terms of order $1/\sqrt{C_0}$ in (A.1) – (A.5) give the following stochastic differential equations for the noise terms.

$$\begin{aligned}
\frac{dX_n(t)}{dt} &= -\lambda_n'(\beta(t))\alpha_n(t)Y(t) - \lambda_n(\beta(t))X_n(t) \\
&\quad -\theta_n(\beta(t))X_g(t)\frac{\alpha_n(t)}{\eta(t)} - \theta_n'(\beta(t))\gamma(t)\frac{\alpha_n(t)}{\eta(t)}Y(t) \\
&\quad -\theta_n(\beta(t))\gamma(t)\left[\frac{1}{\eta(t)}X_n(t) - \frac{\alpha_n(t)}{\eta(t)^2}X_c(t)\right] \\
&\quad -\phi(\beta(t))X_n(t) - \phi'(\beta(t))\alpha_n(t)Y(t) \\
&\quad +\mu(\beta(t))\left[X_c(t) - X_n(t) - X_o(t) - X_g(t)\right] \\
&\quad +\mu'(\beta(t))[\eta(t) - \alpha_n(t) - \alpha_o(t) - \gamma(t)]Y(t) \\
&\quad -\sqrt{\varepsilon\lambda_n(\beta(t))\alpha_n(t)}\,dW_{\lambda_n}(t) - \sqrt{\varepsilon\phi(\beta(t))\alpha_n(t)}\,dW_\phi(t) \\
&\quad -\sqrt{\varepsilon\theta_n(\beta(t))\gamma(t)\frac{\alpha_n(t)}{\eta(t)}}\,dW_{\theta_n}(t) \\
&\quad +\sqrt{\varepsilon 2\mu(\beta(t))(\eta(t) - \alpha_n(t) - \alpha_o(t) - \gamma(t))}\,dW_\mu(t)
\end{aligned} \tag{A.6}$$

$$\frac{dX_o(t)}{dt} = -\lambda_o(\beta(t))\mathbf{X}_o(t) - \lambda_o'(\beta(t))\alpha_o(t)\mathbf{Y}(t)$$

$$-\theta_o(\beta(t))\frac{\alpha_o(t)}{\eta(t)}\mathbf{X}_g(t) - \theta_o'(\beta(t))\gamma(t)\frac{\alpha_o(t)}{\eta(t)}\mathbf{Y}(t)$$

$$-\theta_o(\beta(t))\gamma(t)\left[\frac{1}{\eta(t)}\mathbf{X}_o(t) - \frac{\alpha_o(t)}{\eta(t)^2}\mathbf{X}_c(t)\right] \qquad \text{(A.7)}$$

$$+\phi(\beta(t))\mathbf{X}_n(t) + \phi'(\beta(t))\alpha_n(t)\mathbf{Y}(t)$$

$$-\sqrt{\varepsilon\lambda_o(\beta(t))\alpha_o(t)}\,d\mathbf{W}_{\lambda_o}(t) + \sqrt{\varepsilon\phi(\beta(t))\alpha_n(t)}\,d\mathbf{W}_{\phi}(t)$$

$$-\sqrt{\varepsilon\theta_o(\beta(t))\gamma(t)\frac{\alpha_o(t)}{\eta(t)}}\,d\mathbf{W}_{\theta_o}(t)$$

$$\frac{dX_g(t)}{dt} = -\theta_n(\beta(t))X_g(t)\frac{\alpha_n(t)}{\eta(t)} - \theta_n'(\beta(t))\gamma(t)\frac{\alpha_n(t)}{\eta(t)}Y(t)$$

$$-\theta_n(\beta(t))\gamma(t)\left[\frac{1}{\eta(t)}X_n(t) - \frac{\alpha_n(t)}{\eta(t)^2}X_c(t)\right]$$

$$-\theta_o(\beta(t))X_g(t)\frac{\alpha_o(t)}{\eta(t)} - \theta_o'(\beta(t))\gamma(t)\frac{\alpha_o(t)}{\eta(t)}Y(t)$$

$$-\theta_o(\beta(t))\gamma(t)\left[\frac{1}{\eta(t)}X_o(t) - \frac{\alpha_o(t)}{\eta(t)^2}X_c(t)\right]$$

$$-\xi_n(\beta(t))\alpha_n(t)X_c(t)$$

$$+\xi_n(\beta(t))(1-\eta(t))X_n(t) + \xi_n'(\beta(t))\alpha_n(t)(1-\eta(t))Y(t)$$

$$-\xi_o(\beta(t))\alpha_o(t)X_c(t) + \xi_o(\beta(t))(1-\eta(t))X_o(t)$$

$$+\xi_o'(\beta(t))\alpha_o(t)(1-\eta(t))Y(t)$$

$$+\lambda_o(\beta(t))X_o(t) + \lambda_o'(\beta(t))\alpha_o(t)Y(t)$$

$$+\lambda_n(\beta(t))X_n(t) + \lambda_n'(\beta(t))\alpha_n(t)Y(t) \qquad \text{(A.8)}$$

$$-\sqrt{\varepsilon\theta_n(\beta(t))\gamma(t)\alpha_n(t)/\eta(t)}\,dW_{\theta_n}(t) - \sqrt{\varepsilon\theta_o(\beta(t))\gamma(t)\alpha_o(t)/\eta(t)}\,dW_{\theta_o}(t)$$

$$+\sqrt{\varepsilon\lambda_o(\beta(t))\alpha_o(t)}\,dW_{\lambda_o}(t) + \sqrt{\varepsilon\lambda_n(\beta(t))\alpha_n(t)}\,dW_{\lambda_n}(t)$$

$$+\sqrt{\varepsilon\xi_n(\beta(t))\alpha_n(t)[1-\eta(t)]}\,dW_{\xi_n}(t) + \sqrt{\varepsilon\xi_o(\beta(t))\alpha_o(t)[1-\eta(t)]}\,dW_{\xi_o}(t)$$

$$\frac{dX_c(t)}{dt} = -\xi_o(\beta(t))\alpha_o(t)X_c(t) + \xi_o'(\beta(t))\alpha_o(t)[1-\eta(t)]Y(t)$$

$$+\xi_o(\beta(t))[1-\eta(t)]X_o(t)$$

$$-\xi_n(\beta(t))\alpha_n(t)X_c(t) + \xi_n'(\beta(t))\alpha_n(t)[1-\eta(t)]Y(t)$$

$$+\xi_n(\beta(t))[1-\eta(t)]X_n(t)$$

$$+\sqrt{\varepsilon\xi_o(\beta(t))\alpha_o(t)[1-\eta(t)]}\,dW_{\xi_o}(t) \qquad \text{(A.9)}$$

$$+\sqrt{\varepsilon\xi_n(\beta(t))\alpha_n(t)[1-\eta(t)]}\,dW_{\xi_n}(t)$$

$$\frac{dY(t)}{dt} = \delta_\beta'(\beta(t),\alpha_n(t),\alpha_o(t),\tau(t))Y(t)$$

$$+\delta_{\alpha_n}'(\beta(t),\alpha_n(t),\alpha_o(t),\tau(t))X_n(t)$$

$$+\delta_{\alpha_o}'(\beta(t),\alpha_n(t),\alpha_o(t),\tau(t))X_o(t) \qquad \text{(A.10)}$$

$$+\sigma_T(\beta(t),\alpha_n(t),\alpha_o(t),\tau(t))dW_{\sigma_T}(t)$$

$$+\sigma_\tau\,dW_\tau(t)$$

REFERENCES

L. Arnold, *Stochastic Differential Equations: Theory and Applications.* J. Wiley and Sons, New York, 1974.

A. D. Barbour, "Quasi-stationary distributions in Markov population processes," *Adv. Appl. Prob.*, **8** (1976), pp. 296–314.

L. Bass, P. Robinson, and A. J. Bracken, "Hepatic elimination of flowing substrates: the distributed model," *J. Theoretical Biology*, **72** (1978), pp. 161–184.

F. Y. Bois and P. J. E. Compton-Quintana, "Sensitivity analysis of a new model of carcinogenesis." *J. Theor. Biol.*, **159** (1992), pp. 361–375.

R. L. Carpenter, D. P. Gaver, and P. A. Jacobs, "An exploratory stochastic model for toxic effects on cells," Naval Postgraduate School Technical Report, NPS-OR-93-014, (1993), pp. 1–76.

S. N. Ethier and T. G. Kurtz, *Markov Processes: Characterization and Convergence,* John Wiley and Sons, 1986.

H. I. Freedman and J. B. Shukla, "Models for the effect of toxicant in single-species and predator-prey systems." *J. Math Biology*, **30** (1991), pp. 15–30.

P. Jagers, "Stochastic models for cell kinetics." *Bulletin of Math. Biology*, **45**, No. 4 (1983), pp. 507–519.

R. L. Kodell, D. Krewski, and J. M. Zielinski, "Additive and multiplicative relative risk in the two-stage clonal expansion model of carcinogenesis," *Risk Analysis*, **11** (1991), pp. 483–490.

D. Krewski and C. Franklin (eds.) *Statistics in Toxicology*, Gordon and Breach Science Publishers, New York, 1991.

J. P. Lehoczky and D. P. Gaver, "A diffusion-approximation analysis of a general n-compartment system," *Mathematical Biosciences*, **36** (1977), pp. 127–148.

The Math Works, Inc. *MATLAB Reference Guide*, The Math Works, Inc., Natick, MA, August 1992.

P. McCullagh and J. A. Nelder, *Generalized Linear Models*, Chapman and Hall Ltd., New York, 1983.

D. R. McNeil and S. Schach, "Central limit analogues for Markov population processes," (with discussion), *Journal of the Royal Statistical Soc.*, **1** (1973), pp. 1–23.

S. H. Moolgavkar, A. Dewanji, and D. J. Venzon, "A stochastic two-stage model for cancer risk assessment, I: the hazard function and the probability of tumor." *Risk Analysis*, **8** (1988), pp. 383–392.

P. J. Robinson, A. N. Pettitt, J. Zornig, and L. Bass, "A Bayesian analysis of capillary heterogeneity in the intact pig liver," *Biometrics*, **39** (1983), pp. 61–69.

L. A. Segel and M. Slemrod, "The quasi-steady-state assumption: a case study in perturbation." *SIAM Review*, **31**, No. 3, (1989), pp. 446–477.

INITIAL DISTRIBUTION LIST

1. Research Office (Code 08) 1
   Naval Postgraduate School
   Monterey, CA 93943-5000

2. Dudley Knox Library (Code 52) 2
   Naval Postgraduate School
   Monterey, CA 93943-5002

3. Defense Technical Information Center 2
   Cameron Station
   Alexandria, VA 22314

4. Department of Operations Research (Code OR/Bi) 1
   Naval Postgraduate School
   Monterey, CA 93943-5000

5. Prof. Donald P. Gaver (Code OR/Gv) 10
   Naval Postgraduate School
   Monterey, CA 93943-5000

6. Prof. Patricia A. Jacobs (Code OR/Jc) 5
   Naval Postgraduate School
   Monterey, CA 93943-5000

7. Dr. J. Abrahams, Code 1111, Room 607 1
   Mathematical Sciences Division, Office of Naval Research
   800 North Quincy Street
   Arlington, VA 22217-5000

8. Dr. John Bailar 1
   468 N St. NW
   Washington, DC 20024

9. Dr. David Brillinger 1
   Statistics Department
   University of California
   Berkeley, CA 94720

10. Dr. David Burman 1
AT&T Bell Telephone Laboratories
600 Mountain Avenue
Murray Hill, NJ 07974

11. Prof. Brad Carlin 1
School of Public Health
University of Minnesota
Mayo Bldg. A460
Minneapolis, MN 55455

12. Dr. Robert Carpenter 1
NAMRI/Navy Toxicology Detachment
Bldg. 433, Area B
Wright-Patterson AFB, OH 45433-6503

13. Center for Naval Analyses 1
4401 Ford Avenue
Alexandria, VA 22302-0268

14. Dr. Edward G. Coffman, Jr. 1
AT&T Bell Telephone Laboratories
600 Mountain Avenue
Murray Hill, NJ 07974

15. Professor Sir David Cox 1
Nuffield College
Oxford, OXI INF
ENGLAND

16. Professor H. G. Daellenbach 1
Department of Operations Research
University of Canterbury
Christchurch, NEW ZEALAND

17. Dr. D. F. Daley 1
Statistic Dept. (I.A.S.)
Australian National University
Canberra, A.C.T. 2606
AUSTRALIA

18. Dr. Naihua Duan 1
RAND Corporation
Santa Monica, CA 90406

19. Prof. Bradley Efron 1
Statistics Dept.
Sequoia Hall
Stanford University
Stanford, CA 94305

20. Prof. George S. Fishman 1
Curr. in OR & Systems Analysis
University of North Carolina
Chapel Hill, NC 20742

21. Henry S. Gardner 1
U.S. Army Biological Research & Development Laboratory
Ft. Detrick, MD 21702-5010

22. Dr. Andrew Gelman 1
Statistics Dept.
University of California
Berkeley, CA 94720

23. Dr. Neil Gerr 1
Office of Naval Research
Arlington, VA 22217

24. Prof. Peter Glynn 1
Dept. of Operations Research
Stanford University
Stanford, CA 94350

25. Prof. Linda V. Green 1
Graduate School of Business
Columbia University
New York, NY 10027

26. Prof. J. Michael Harrison 1
Graduate School of Business
Stanford University
Stanford, CA 94305-5015

27. Dr. P. Heidelberger 1
IBM Research Laboratory
Yorktown Heights
New York, NY 10598

28. Dr. D. C. Hoaglin 1
Department of Statistics
Harvard University
1 Oxford Street
Cambridge, MA 02138

29. Prof. D. L. Iglehart 1
Dept. of Operations Research
Stanford University
Stanford, CA 94350

30. Institute for Defense Analysis 1
1800 North Beauregard
Alexandria, VA 22311

31. Prof. J. B. Kadane 1
Dept. of Statistics
Carnegie-Mellon University
Pittsburgh, PA 15213

32. Dr. F. P. Kelly 1
Statistics Laboratory
16 Mill Lane
Cambridge
ENGLAND

33. Dr. Jon Kettenring 1
Bellcore
445 South Street
Morris Township, NJ 07962-1910

34. Koh Peng Kong 1
OA Branch, DSO
Ministry of Defense
Blk 29 Middlesex Road
SINGAPORE 1024

35. Prof. Guy Latouche 1
University Libre Bruxelles
C.P. 212, Blvd. De Triomphe
B-1050 Bruxelles
BELGIUM

36. Dr. A. J. Lawrence 1
Dept. of Mathematics,
University of Birmingham
P. O. Box 363
Birmingham B15 2TT
ENGLAND

37. Prof. M. Leadbetter 1
Department of Statistics
University of North Carolina
Chapel Hill, NC 27514

38. Prof. J. Lehoczky 1
Department of Statistics
Carnegie-Mellon University
Pittsburgh, PA 15213

39. Dr. Colin Mallows 1
AT&T Bell Telephone Laboratories
600 Mountain Avenue
Murray Hill, NJ 07974

40. Dr. Sati Mazumdar 1
Biostatistics Dept.
University of Pittsburgh
Graduate School of Public Health
Pittsburgh, PA 15261

41. Dr. James McKenna 1
Bell Communications Research
445 South Street
Morristown, NJ 07960-1910

42. Prof. Carl N. Morris 1
Statistics Department
Harvard University
1 Oxford St.
Cambridge, MA 02138

43. Dr. John A. Morrison 1
AT&T Bell Telephone Laboratories
600 Mountain Avenue
Murray Hill, NJ 07974

44. Prof. F. W. Mosteller 1
Department of Statistics
Harvard University
1 Oxford St.
Cambridge, MA 02138

45. Operations Research Center, Rm E40-164 1
Massachusetts Institute of Technology
Attn: R. C. Larson and J. F. Shapiro
Cambridge, MA 02139

46. Dr. John Orav 1
Biostatistics Department
Harvard School of Public Health
677 Huntington Ave.
Boston, MA 02115

47. Dr. Jim Petty 1
National Biological Survey
4200 New Haven Road
Columbia, MO 65201

48. Dr. V. Ramaswami 1
MRE 2Q-358
Bell Communications Research, Inc.
445 South Street
Morristown, NJ 07960

49. Dr. Martin Reiman 1
Rm #2C-117
AT&T Bell labs
600 Mountain Ave.
Murray Hill, NJ 07974-2040

50. Dr. Lorenz Rhomberg 1
Harvard Center for Risk Analysis
Harvard University
Cambridge, MA 02138

51. Prof. Maria Rieders 1
Dept. of Industrial Eng.
Northwestern Univ.
Evanston, IL 60208

52. Dr. John E. Rolph 1
RAND Corporation
1700 Main St.
Santa Monica, CA 90406

53. Prof. Frank Samaniego 1
Statistics Department
University of California
Davis, CA 95616

54. Prof. W. R. Schucany 1
Dept. of Statistics
Southern Methodist University
Dallas, TX 75222

55. Prof. D. C. Siegmund 1
Dept. of Statistics
Sequoia Hall
Stanford University
Stanford, CA 94305

56. Prof. H. Solomon 1
Department of Statistics
Sequoia Hall
Stanford University
Stanford, CA 94305

57. Andrew Solow 1
Woods Hole Oceanographic Institute
Woods Hole, MA 02543

58. Prof. W. Stuetzle 1
Department of Statistics
University of Washington
Seattle, WA 98195

59. Dr. D. J. Svensgaard 1
Health Effects Research Lab
U. S. Environmental Protection Agency
Biostatistics Branch MD55
Research Triangle Park, NC 27711

60. Prof. J. R. Thompson 1
Dept. of Mathematical Science
Rice University
Houston, TX 77001

61. Prof. J. W. Tukey 1
Statistics Dept., Fine Hall
Princeton University
Princeton, NJ 08540

62. Dr. D. Vere-Jones 1
Dept. of Math, Victoria Univ. of Wellington
P. O. Box 196
Wellington
NEW ZEALAND

63. Prof. David L. Wallace 1
Statistics Dept., University of Chicago
5734 S. University Ave.
Chicago, IL 60637

64. Dr. Ed Wegman 1
George Mason University
Fairfax, VA 22030

65. Dr. Alan Weiss 1
Rm. 2C-118
AT&T Bell Laboratories
600 Mountain Avenue
Murray Hill, NJ 07974-2040

66. Dr. P. Welch 1
IBM Research Laboratory
Yorktown Heights, NY 10598

67. Prof. Roy Welsch 1
Sloan School
M.I.T.
Cambridge, MA 02139

68. Dr. Tandore Narayanan 1
NAMRI/Navy Toxicology Detachment
Bldg. 433, Area B
Wright-Patterson AFB, OH 45433-6503